# Surficial Geology

## Regolith mapping using integrated Landsat TM imagery and high resolution gamma-ray spectrometric imagery — Cape York Peninsula

3

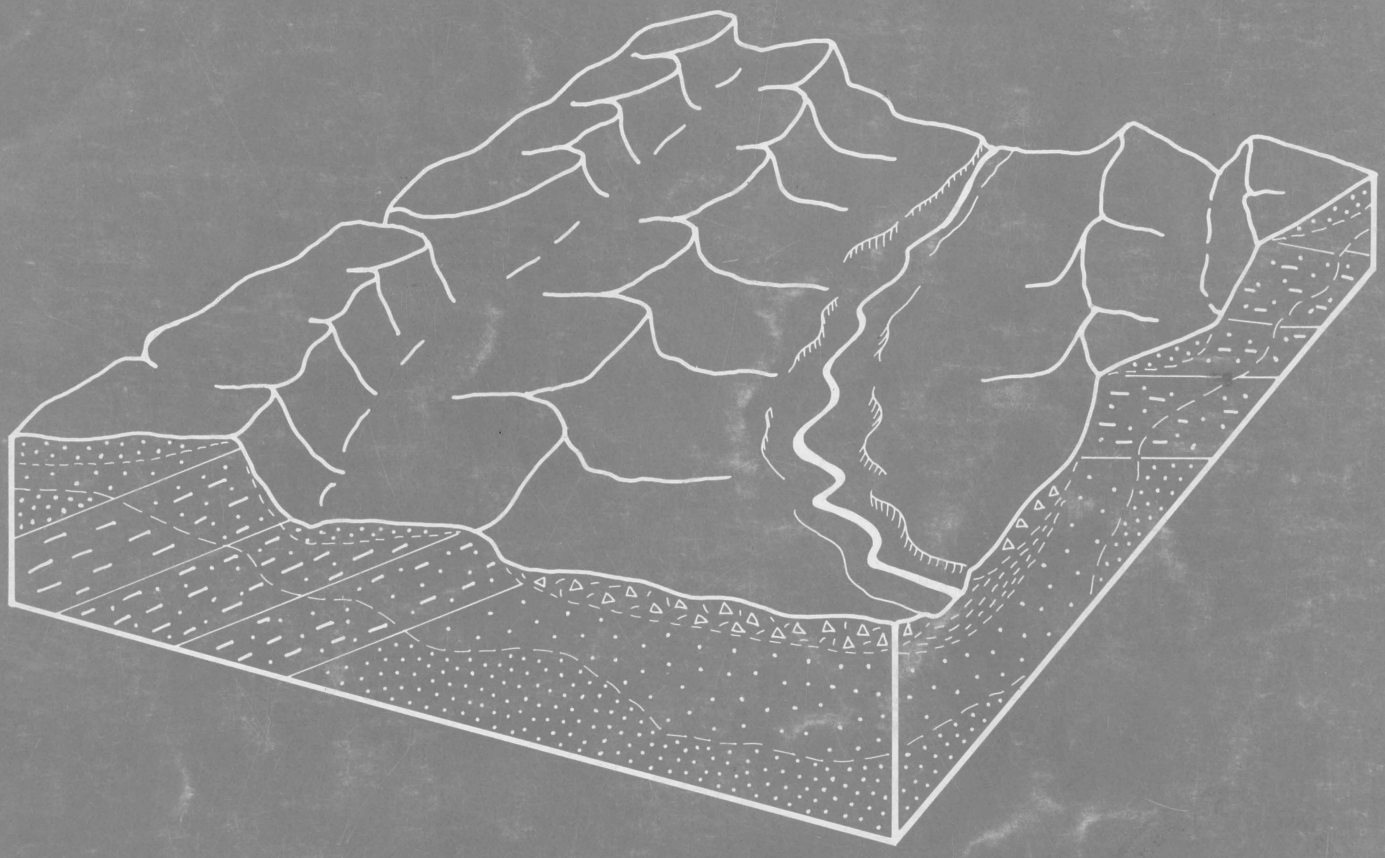



Record 1992/78

by J R Wilford



BMR
GEOLOGY AND
GEOPHYSICS
AUSTRALIA

*Minerals and Land Use Program*

YSICS

# Regolith mapping using integrated Landsat TM imagery and high resolution gamma-ray spectrometric imagery — Cape York Peninsula

3

A contribution to the National Geoscience Mapping Accord
NORTH QUEENSLAND PROJECT

AGSO
AUSTRALIAN GEOLOGICAL SURVEY ORGANISATION

DEPARTMENT OF RESOURCE INDUSTRIES



**Record 1992/78**

**by J R Wilford**

*Minerals and Land Use Program*

**DEPARTMENT OF PRIMARY INDUSTRIES AND ENERGY**
Minister for Resources: The Hon. Alan Griffiths
Secretary: Geoff Miller

AUSTRALIAN GEOLOGICAL SURVEY ORGANISATION
(formerly BUREAU OF MINERAL RESOURCES, GEOLOGY AND GEOPHYSICS)

Executive Director: Roye Rutland

**DEPARTMENT OF MINERALS AND ENERGY**
**(formerly DEPARTMENT OF RESOURCES INDUSTRIES, QUEENSLAND)**
Minister: The Hon. Tony McGrady
Director-General: P. Breslin

GEOLOGICAL SURVEY OF QUEENSLAND

Chief Government Geologist: R.W.Day



ISSN 0811-062X
ISBN 0 642 18440 2

# TABLE OF CONTENTS

## FIGURES



## TABLES

# ABSTRACT

High-resolution (400m line spacing) airborne gamma-ray data gathered for the National Geoscience Mapping Accord North Queensland Project has proved invaluable for differentiating between regolith types based on their potassium, thorium and uranium signatures. The ability of the gamma-ray signal to "see through" the vegetation cover and as much as 40cm below the surface was a considerable advantage in north Queensland where other remote sensing data sets (e.g. Landsat TM) are hindered by the thick vegetation cover, and where much of the underlying geology is masked by residual sandy soils.

Two image processing techniques were used to enhance the gamma-ray data and integrate it with Landsat TM data. Firstly, the hillshaded (high frequency component) of the gamma-ray data was added to a three-band false-colour composite image of the corrected gamma-ray data. The hillshaded component highlighted local changes in the gamma-ray signal which related to changes in regolith materials and lithology, and sharpened boundaries associated with geomorphic features. Secondly, the gamma-ray image was then combined (pixel by pixel) with the high frequency component of a Landsat TM (band 5) scene. This allowed the imagery to be interpreted in a geomorphological and structural context.

Broad lithological divisions and structural domains were identified in the imagery, but most of the variation within these groups relates to the regolith cover and to geomorphic features in the landscape. Subtle variations in lithology were effectively interpreted only when the responses of the regolith cover were known. The gamma-ray imagery provided an insight into the weathering and geomorphic history of the region. In addition, the imagery can also be interpreted as a 'geomorphic activity map', separating stable landforms with deep weathering from younger landforms with active erosion and stripping of the surficial cover. This allows past and present geomorphic processes to be interpreted from the imagery, which in turn provides more informed extrapolation of field results and prediction of regolith types.

The integrated imagery proved particularly useful for regolith mapping. There is considerable potential for assisting with interpretation of both stream-sediment geochemical data and environmental studies, because the imagery effectively maps the distribution of sediments and soils in the landscape, and identifies areas of erosion and land degradation.

# 1 INTRODUCTION

The use of gamma-ray spectrometric data for bedrock mapping is well documented and understood (Darnley & Grasty 1971, Foote & Humphrey 1976, and Tucker & others, 1984). However, there has been relatively little work on the use of such data for mapping regolith. This record is a contribution to the latter.

## 1.1 The Project

This study is a contribution of the National Geoscience Mapping Accord (NGMA) North Queensland Project being carried out jointly by the Australian Geological Survey Organisation (AGSO) and the Queensland Department of Minerals and Energy. The project aims to produce second-generation geophysical and geological maps of north Queensland to provide an up-to-data data base for, among other things, a detailed resource assessment of the area. Reconnaissance regolith–landform maps at a scale of 1:250 000 are being produced as part of the NGMA project.

Regolith consists of both transported and *in situ* weathered materials overlying bedrock. Methods for characterising and mapping these materials developed at AGSO (Pain & others, 1991, Pain, 1992), rely to a large extent on recognition of the close relationships between regolith and landforms; landforms are used as a surrogate for regolith materials when mapping at reconnaissance scales. However, gamma-ray spectrometric images were recognised as an important data source to complement regolith information obtained from landform distribution, and field observations (Bain & others, 1992). This recognition is the basis of the work presented in this report.

## 1.2 Objectives

This report describes the processing, enhancement and interpretation of Landsat TM Thematic Mapper (TM) and airborne gamma-ray spectrometric imagery of the Ebagoola 1:250 000 sheet area in north Queensland for regolith–landform mapping and interpretation. Specific objectives (of the report) are:

- To document the methodology for the processing of Landsat TM and airborne gamma-ray spectrometric imagery to enhance landform–regolith information.
- To present an initial interpretation of airborne gamma-ray spectrometric responses to regolith materials.
- To illustrate the use of Landsat TM and airborne gamma-ray spectrometric imagery for regolith–landform mapping of the Ebagoola 1:250 000 sheet area (SD54–12).

## 1.3 Regolith–landform concepts

Regolith–landform maps provide information on the character and distribution of weathered materials, terrestrial sediments and landforms. Regolith mapping units are generally much thinner, more variable and discontinuous than bedrock units, and therefore require a different approach to mapping. Landform mapping has been used as a surrogate for regolith mapping, because there is a very close relationship between landforms and the distribution and type of regolith. A regolith–landform unit consists of one, or more usually several, recurring landscape

elements and associated regolith packages which together form a distinct regolith–landform entity (Pain & others, 1991). This landscape approach to regolith mapping is described by Pain (1992).

Three principal applications of regolith–landform mapping are to:

- provide insights into, and correlations between, the weathered surface and underlying bedrock geology and mineral deposits;
- map the distribution of regolith types of economic potential (e.g. bauxite); and
- provide information for land-use issues, including land suitability, soil degradation and environmental fragility.

## 1.4 Study area

The Ebagoola 1:250 000 sheet area (EBAGOOLA) lies between latitudes 14° and 15° S, and longitudes 142°–30' and 144°E on the east coast of Cape York Peninsula (Fig. 1). It has a monsoonal climate with distinct dry and wet seasons. The wettest months occur between November and April and account for 95 % of the annual rainfall. Average annual rainfall based on records from the township of Coen 8 km north of the sheet area is 1117mm. During the summer months maximum temperatures typically fall within the range of 32–35°C, and winter temperatures are 5–6 degrees cooler. Vegetation consists of mangroves, salt-tolerant halophytic grasses and shrubs on tidal mud flats and estuaries along the east coast, *Melaleuca viridiflora* woodlands on low-relief alluvial plains and areas prone to water logging, and *Eucalyptus* open forests and woodlands on undulating, well drained areas.

The bedrock consists of a central core of folded metamorphic rocks and Palaeozoic granites, known as the Coen Inlier (Fig.1) (Whitaker & Gibson, 1977). Gently dipping Mesozoic sediments of the Carpentaria and Laura Basins flank the Inlier to the west and east respectively. Cainozoic fluvial sediments occur on granite and metamorphic terrains but are most common over Mesozoic sediments. Recent geological mapping of EBAGOOLA has further subdivided the rock units and revised the lithological, structural and deformational history of the region. As a result of the NGMA mapping a revised geological map of the area with accompanying explanatory notes has been published (Ewers & Bain, 1992).

# 2 DATA AND IMAGE REGISTRATION

To facilitate geological and regolith landform mapping of the EBAGOOLA map sheet area remotely sensed data sets including Landsat TM (band 5) and a standard false colour composite image of the gamma-ray data (red=potassium, green=thorium & blue=uranium) were produced at 1:100 000 scale and geo-referenced to the Australian Map Grid (AMG).

## 2.1 Gamma-ray spectrometric data

The (high resolution) airborne gamma-ray spectrometric data were digitally recorded and processed by Geoterrex Pty Ltd in October/November 1991, under contract to the AGSO Geophysical Observatories and Mapping Program. The data were recorded at a flight altitude of 100m above the ground, with a flightline spacing of 400m, and a sampling interval along line of 70m. The gamma-ray spectrometer measures the gamma-ray spectrum in 256 channels over the energy range of 0.4 to 3.0 MeV. Gamma-ray windows most suitable for measuring potassium,

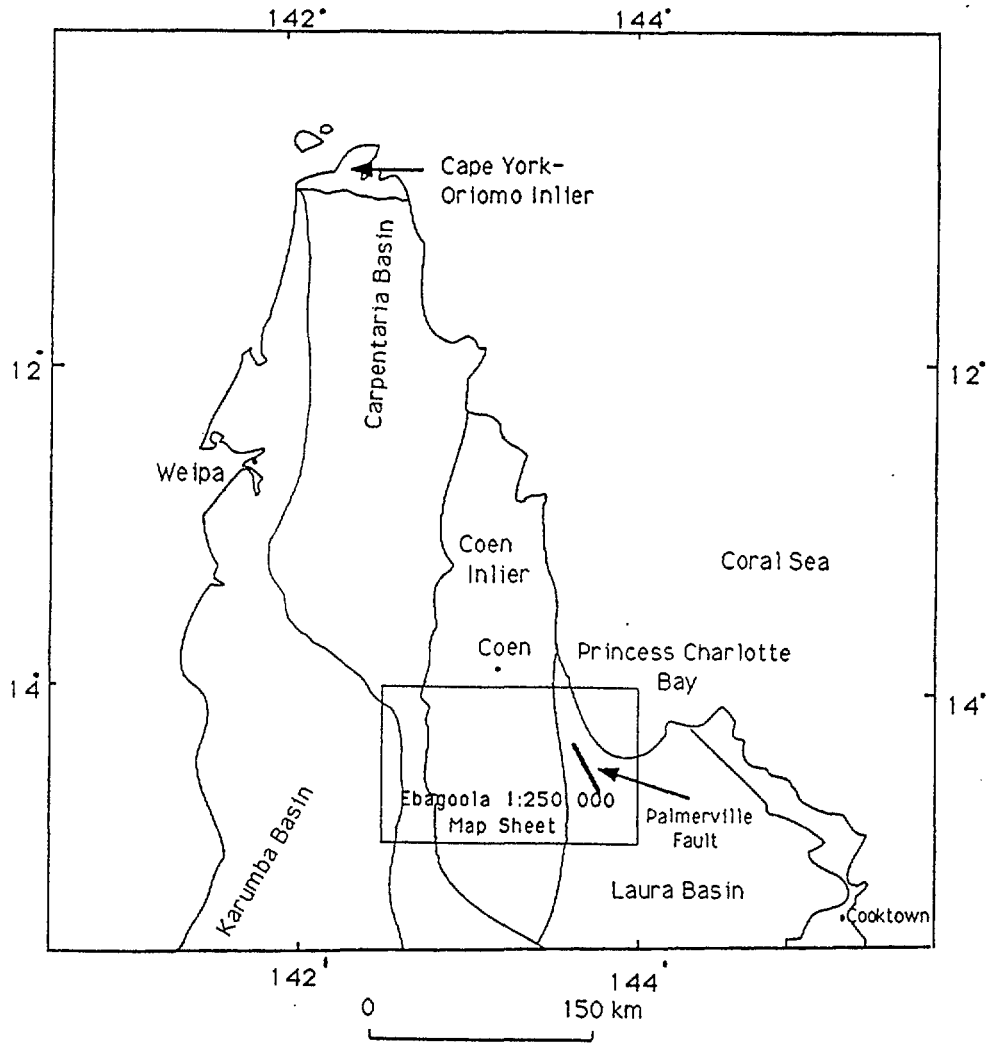


**Figure 1. Location of the EBAGOOLA map sheet study area.**

uranium and thorium are: 1.46 MeV corresponding to the isotopic decay peak of potassium-40 for potassium, 1.76MeV corresponding to the isotopic decay peak of bismuth-214 for uranium, and 2.62 MeV corresponding to the isotopic decay peak of thallium-208 for thorium (Grasty, 1976) (Fig. 2). The source of gamma-ray radiation for potassium relates directly to common rock forming minerals (e.g. feldspars, mica) and clays (e.g. illite). Sources of uranium and thorium radiation are concentrated in accessory minerals such as zircon, titanite, monazite, allanite, pyrochlore, xenotime, uraninite and thorite (Table 1). Corrections were made for Compton scattering, height attenuation and changes in ambient air temperature (Geoterrex, 1991). The sampling area of the gamma-ray spectrometer is typically expressed as the diameter of a circle, and depends on the flying height of the aircraft and the energy level of gamma radiation. The EBAGOOLA gamma-ray data have a diameter zone of influence or ground resolution of 400m (Geoterrex, 1991).

The data were gridded by Geophysical Observatories and Mapping Program of AGSO using a minimum curvature gridding algorithm described by Briggs (1974). Striping and background noise in the image were removed using two algorithms. The first called 'Ulevel' corrects the uranium band for poor background removal using an interchannel correlation method which operates on the line data (Green, 1987). The second called 'Gfilt' (developed by the Geophysical Observatories and Mapping Program AGSO) uses a one-dimensional filter on rows (pixels) and columns (lines) on each gridded channel to remove spurious elongate artefacts. Once gridded,

| Mineral | Nominal composition | Radioactive element abundances[a] | | |
|---|---|---|---|---|
| | | K | U | Th |
| Adularia | $KAlSi_3O_8$ | 14.0 | — | — |
| Allanite | $(Ca,X)_2(Al,Fe,Mg)_3Si_3O_{12}(OH)$ | — | * | *** |
| Alunite | $KAl_3(SO_4)_2(OH)_6$ | 9.4 | — | — |
| Apatite | $Ca_5(PO_4)_3(F,Cl,OH)$ | — | * | * |
| Apophyllite | $KCa_4(Si_4O_{10})_2F{\cdot}8H_2O$ | 4.1 | — | — |
| Autunite | $Ca(UO_2)_2(PO_4)_2{\cdot}10–12H_2O$ | — | 48–50 | — |
| Biotite | $K(Mg,Fe)_3(AlSi_3O_{10})(OH)_2$ | 8–9 | — | — |
| Carnallite | $KMgCl_3{\cdot}6H_2O$ | 14.1 | — | — |
| Carnotite | $K_2(UO_2)_2(VO_4)_2{\cdot}3H_2O$ | 7.2 | 53 | — |
| Glauconite | Complex sheet silicate | 4.6–6.2 | — | — |
| Hornblende | $NaCa_2(Mg,Fe,Al)_5(Si,Al)_8O_{22}(OH)_2$ | *** | — | — |
| Lepidolite | Lithium mica | 7.1–8.3 | — | — |
| Leucite | $KAlSi_2O_6$ | 17.9 | — | — |
| Microcline | $KAlSi_3O_8$ | 14.0 | — | — |
| Monazite | $(Ce,La,Y,Th)PO_4$ | — | ** | 2–20 |
| Muscovite | $KAl_2(AlSi_3O_{10})(OH)_2$ | 9.8 | — | — |
| Nepheline | $(Na,K)AlSiO_4$ | 3–10 | — | — |
| Orthoclase | $KAlSi_3O_8$ | 14.0 | — | — |
| Phlogopite | $KMg_3(AlSi_3O_{10})(OH)_2$ | 9.4 | — | — |
| Pitchblende | Massive $UO_2$ | — | 88 | — |
| Polyhalite | $K_2Ca_2Mg(SO_4)_4{\cdot}2H_2O$ | 13.0 | — | — |
| Sanidine | $KAlSi_3O_8$ | 14.0 | — | — |
| Sphene | $CaTiSiO_5$ | — | * | * |
| Sylvite | KCl | 52.4 | — | — |
| Thorianite | $ThO_2$ | — | — | 88 |
| Thorite | $ThSiO_4$ | — | *** | 72 |
| Torbernite | $Cu(UO_2)(PO_4)_2{\cdot}8–12H_2O$ | — | 32–36 | — |
| Tyuyamunite | $Ca(UO_2)_2(VO_4)_2{\cdot}5–8^1/_2H_2O$ | — | 45–48 | — |
| Uraninite | $UO_2$ | — | 88 | — |
| Xenotime | $YPO_4$ | — | *** | ** |
| Zircon | $ZrSiO_4$ | — | ** | ** |

[a] Abundances in percents except as noted: ***, 0.5—3% range, **, 0.1—0.5% range, *, 0.001—0.1% range.

**Table 1. The major naturally occurring radioactive minerals (from Van Schmus,1984).**

the data can be enhanced, geocoded and integrated with other raster data sets in an image processing system.

Airborne gamma-ray spectrometric profiles of potassium, thorium and uranium flown from east to west were also utilized for interpretation. The gamma-ray spectrometric profiles represent the original gamma-ray profiles obtained from the survey and measure counts per second for potassium, thorium and uranium. Gamma-ray spectrometric profiles record data at 70m intervals along the line and consequently contained more subtle information than the imaged data which has been smoothed in the gridding process to accommodate the 400m line spacing.

## 2.2 Landsat Thematic Mapper (TM)

Landsat Thematic Mapper (TM) records data in seven spectral bands, six in the visible and reflected infrared part of the electromagnetic spectrum with a spatial resolution of 30m by 30m

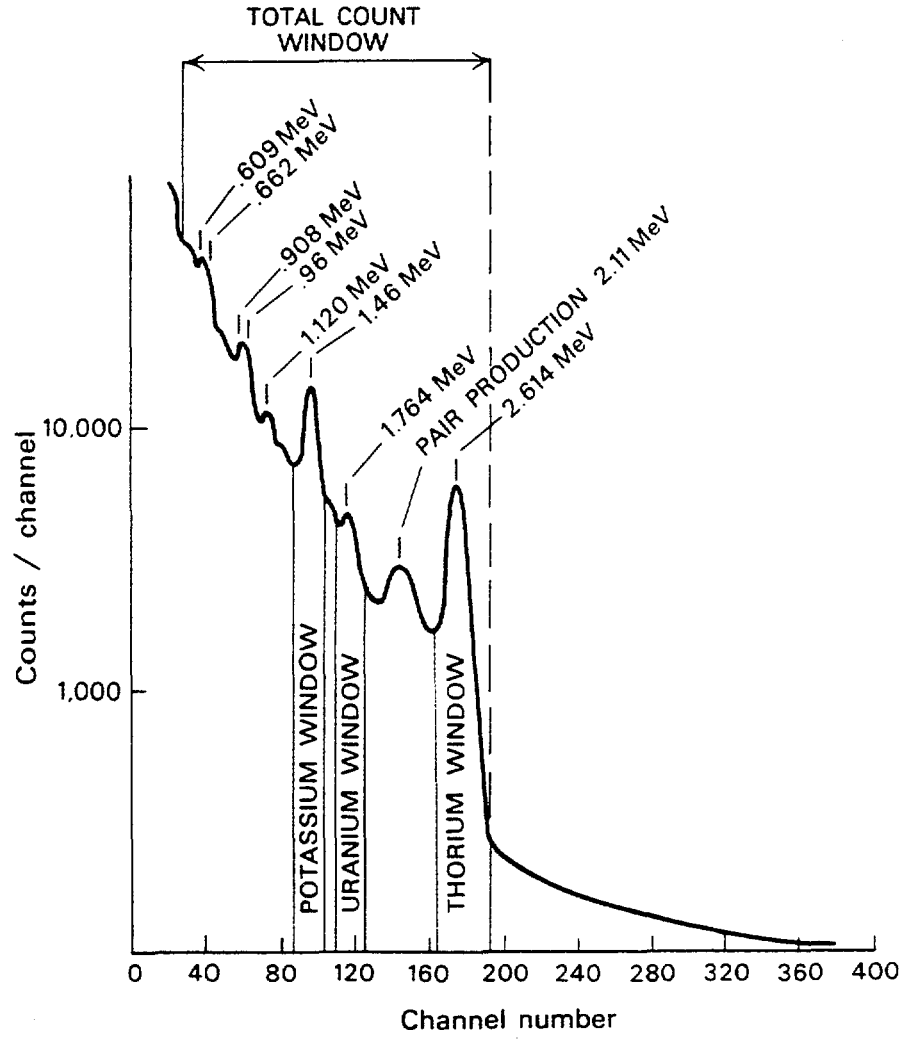


**Figure 2 Gamma-ray spectrum showing the main photopeaks and channel positions for potassium, uranium and thorium (modified from Foote, 1968).**

(pixels) and one in the thermal infrared region with a pixel resolution of 120m by 120m. Band 5 (1.55-1.75μm infrared radiation ) of TM was the only band used in the investigation and was chosen in preference to other bands because its high spectral reflectance peak of rock materials records the sharpest definition of rock boundaries for discriminating landforms and structural features.

To provide a complete satellite coverage over EBAGOOLA two TM scenes, path/rows 98/70 and 97/70 were joined together. Cape York Peninsula is frequently cloud covered, and the best cloud-free imagery for these path/row scenes were recorded one and a half years apart (6/4/88 and 3/11/86, respectively). There were thus clear differences in vegetation cover between the scenes, mainly reflecting phenological variations and fireburn. To compensate for these variations the histograms of the two scenes were matched, effectively normalising the spectral differences between them. This proved to be quite successful, although the join in the combined image can still be seen in places.

## 2.3 Geometric corrections

The TM and gamma-ray images were geometrically registered to allow them to be correlated and integrated. The data sets were warped to a common scale and map projection—the Australian Map Grid (AMG). A second order polynomial fit based on 15 ground control points was used to warp and re-sample the TM image to 50m pixels. Road intersections and drainage junctions

which can be readily and accurately located on the imagery and on topographic maps were used as ground-control points. The airborne gamma-ray data were converted from latitude and longitude coordinates to the AMG and re-sampled to 50m pixels using 10 control points. A nearest neighbour re-sampling technique was used to generate 50m pixels to match the resolution of the satellite imagery whilst maintaining the spectral integrity of the data.

# 3 DATA PROCESSING AND INTEGRATION

A variety of image processing and integration techniques were used to enhance the imagery and combine the complementary components of the gamma-ray and Landsat TM data sets.

## 3.1 Data processing

Various image enhancement techniques were applied to the gamma-ray data in attempts to discriminate between lithologies and regolith materials throughout the sheet area. These techniques including principal component analysis, spatial filtering, ratioing bands, false-colour linear stretches and pre-classification (unsupervised) algorithms (Drury, 1987). The principal component analysis, although producing effective colour separation, was difficult to interpret due to the band-mixing involved. Unsupervised classification using a minimum distance algorithm was effective in clustering the three-channel gamma-ray data into classes with similar gamma-ray characteristics. Clustering required smoothing of the original data to produce clusters that are less 'noisy' and easier to classify. This produced a simplified image for interpretation. However, the standard 3 band false-colour composite image of potassium in red, thorium in green and uranium in blue was found to be the most effective display for discriminating and interpreting surface materials. The false-colour composite rendition, displayed with a linear stretch, preserved the original integrity of the data, allowing relative proportions of potassium, thorium and uranium to be directly related to surface materials. The image was further enhanced by adding back a hillshaded (a high band-pass filter with an east/west artificial sun-angle illumination) component of the gamma-ray data to a three-band false-colour composite image using a pixel by pixel additive method (Fig. 3). The hillshaded gamma-ray image highlighted boundaries related to the distribution of surface materials (Fig. 4a).

## 3.2 Integration

Two techniques were used to combine the Landsat TM band 5 scene with the gamma-ray image:

- The colour model (Foley & others, 1990) using hue, saturation and value (HSV) was used to merge data sets. Once the data sets are converted into HSV colour space, each of the colour parameters can be exchanged with other registered data sets to integrate them. In this case, the value component of the gamma-ray image was replaced by TM band 5 before the image was converted back to the original red, blue and green (RGB) colour coordinate system for display. This method distorts to various degrees the spectral characteristics of the original gamma-ray image, thus impeding interpretation.
- Hillshading the TM scene with an east-west artificial illumination removes areas of continuous tone which would otherwise distort the spectral integrity of the gamma-ray image. The hillshaded image highlights the high-frequency component of the image

which displays landform, structural features and drainage patterns whilst removing the tonal component of the original image (i.e. uniformly dark areas reflecting dense vegetation cover or bright areas reflecting exposed soil) which would otherwise distort the spectral characteristic of the gamma-ray image. Pixel-by-pixel adding was the most effective way of combining the hillshaded TM scene with the gamma-ray data (Fig. 3). This allows complete control on the percentage of each pixel added from each data set to the combined image. The combined image effectively incorporates the high spatial resolution of the TM data while preserving the spectral integrity of the gamma-ray image (Fig. 4b). The hillshade algorithm operates in a similar manner to a directional high-pass filter (Convolution Kernel for east-west directional filter is shown below).

—1 0 1
—1 0 1
—1 0 1

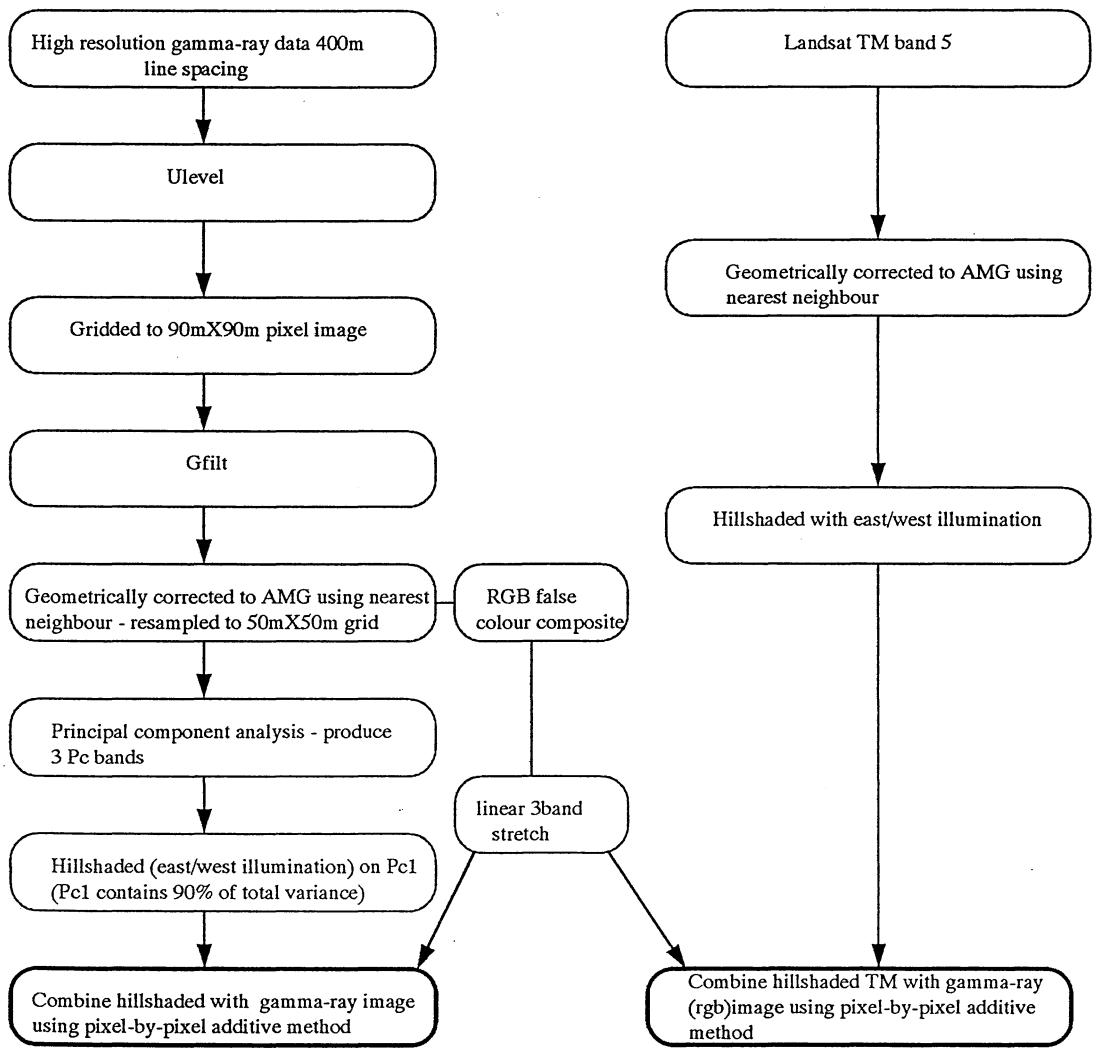


**Figure 3. Flow chart showing the steps involved in processing and integrating the gamma-ray and Landsat TM data.**

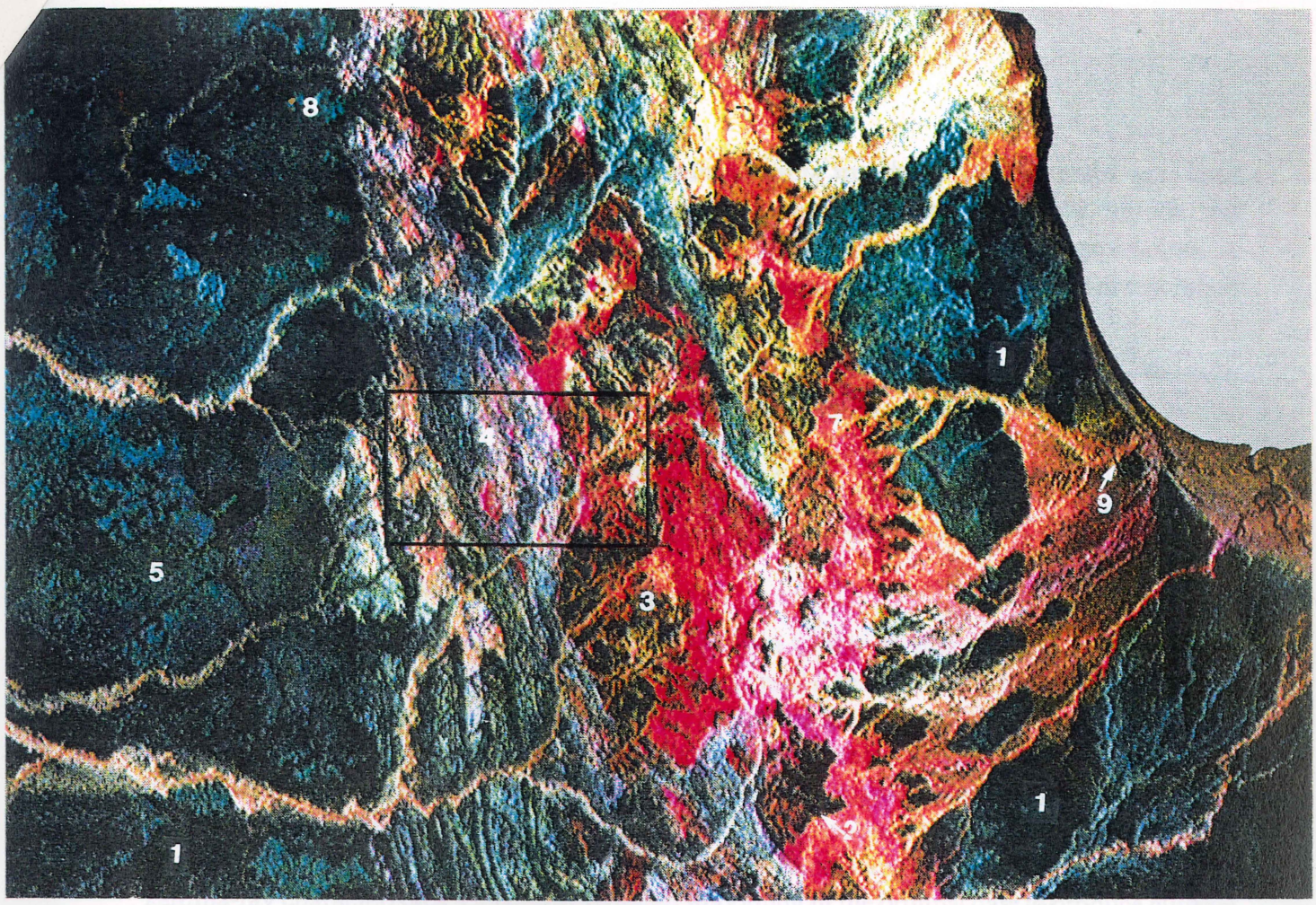


(a)

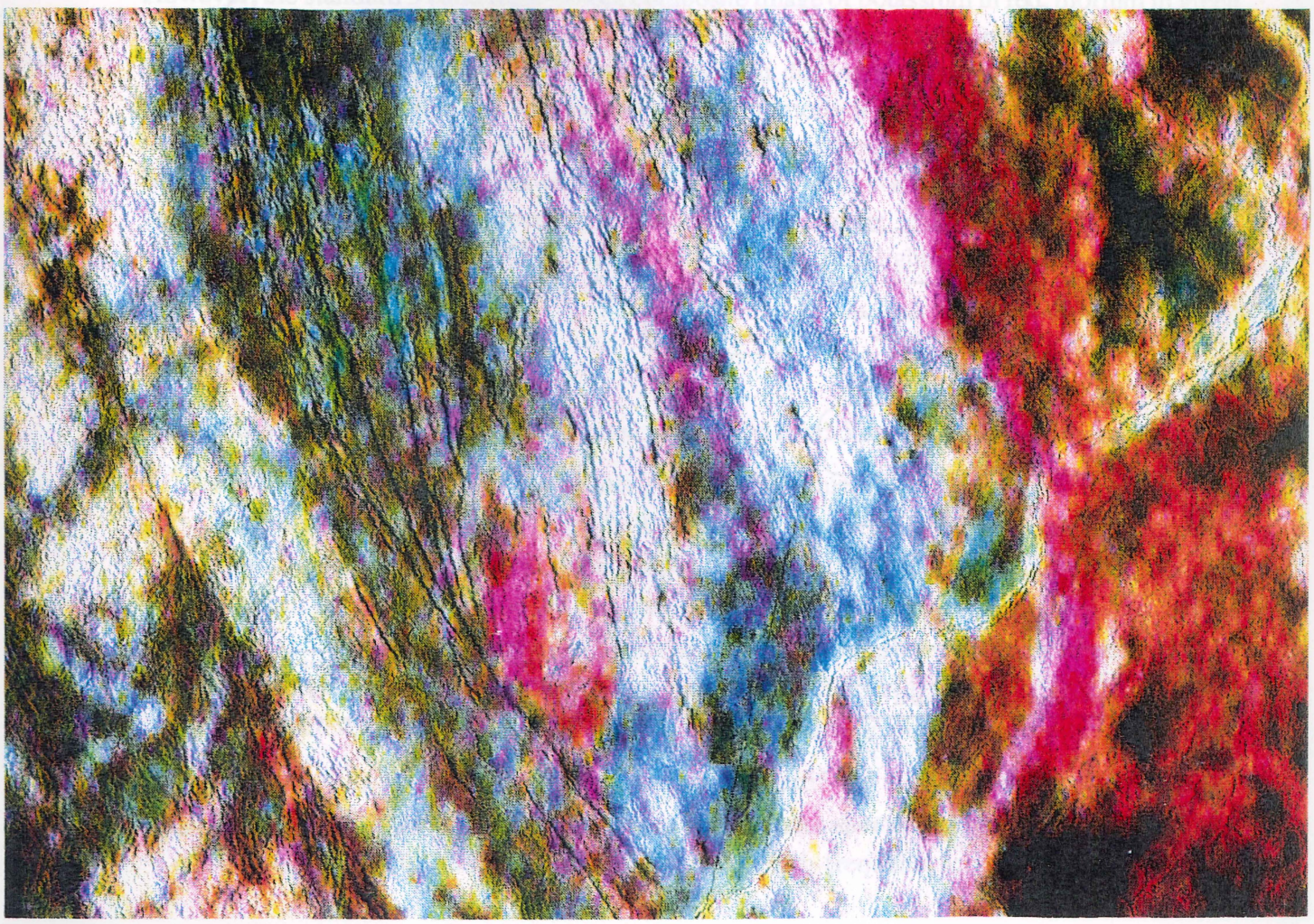

(b)

**Figure 4. (a) (Opposite page) Three band gamma-ray spectrometric image (potassium=red, thorium=green and uranium=blue) with hillshaded high frequency component added back; over the Ebagoola 1:250 000 sheet. 1 = residual sand, 2 = edge of Great Escarpment, 3 = soils on granites, 4 = soils on metamorphics, 5 = soils on sandstone & siltstone, 6 = erosion associated with river capture, 7 = active erosion, 8 = bauxitic soils, 8 = area of relief inversion and 9 = beach strand-line. (refer to text for descriptions) Box center of image shows location of sub-scene below. (b) Sub-scene of combined hillshaded Landsat TM band 5 image with gamma-ray data. The high spatial resolution of the TM scene highlights structural and landform features whilst the gamma-ray data provide information on surface chemistry. Superimposed drainage of the Lukin River can been seen cutting across steep strike slip ridges of quartzite (blue/green hues).**

Two gamma-ray enhancements derived from these image processing and integration techniques were used for interpretation: (1) a hillshaded gamma-ray image (Fig. 4a) and (2) a combined Landsat TM/ gamma-ray image (Fig. 4b). Landsat TM band 5 was also used in conjunction with aerial photography to map structure and morphotectonic elements and to classify landforms over the region.

# 4 REGOLITH OVERVIEW

The main geomorphic feature of the area is the Great Escarpment (Ollier, 1982), which crosses the sheet area from north to south (Fig. 5). The regolith is mainly *in situ* weathered bedrock (Bain & others, 1992). Transported material covers only a small part of the sheet area, occurring as alluvial, colluvial and coastal sediments east of the Great Escarpment and major channel and overbank deposits associated with rivers flowing west to the Gulf of Carpentaria. The distribution of *in situ* weathered regolith and transported sediments is shown in Figure 5. Regolith distribution appears to reflect more-or-less continuous denudation since the retreat of the sea in the mid Cretaceous. Three broad regolith-landform associations are recognised, coinciding with the major physiographic units of Whitaker & Gibson, (1977). These are the Coastal Plain, the Central Uplands and the Western Plains (Fig.5). The Coastal and Western plains are flat to gently undulating with low relief (generally 30m). The Central Uplands are higher in elevation and vary from low hills to steep hills and ridges with deeply incised valleys (local relief up to 160m) (Fig.6).

## 4.1 The Coastal Plains

The Coastal Plains (Fig. 5) are characterised by alluvial, coastal and aeolian sediments. The coastline is fringed by sand dunes and linear beach ridges interrupted in places by low sandstone cliffs of the Mesozoic Gilbert River Formation. Supratidal plains with clay flats and saltpans occur immediately inland. The plains consist of lagoonal and estuarine silts and clays drained by sinuous tidal creeks fringed with mangroves. In the southeastern corner of the map sheet, sediments from the major rivers (North Kennedy and Annie) have built up a broad coastal depositional plain. The plain is characterised by meandering channels with point-bar deposits, oxbow lagoons, mudflats, saltpans and tidal creeks. Vegetation on the plain is either absent or consists of salt-tolerant halophytic grasses and shrubs. Mangroves form a dense canopy lining the tidal creeks and rivers. Further inland (up to 15km from the present coast line), beach sand deposits indicate an older strandline probably formed during the last interglacial when eustatic sea level was higher. The beach deposits are preserved either as long, narrow, sandy ridges, or as scattered residual ridges truncated by numerous streams.

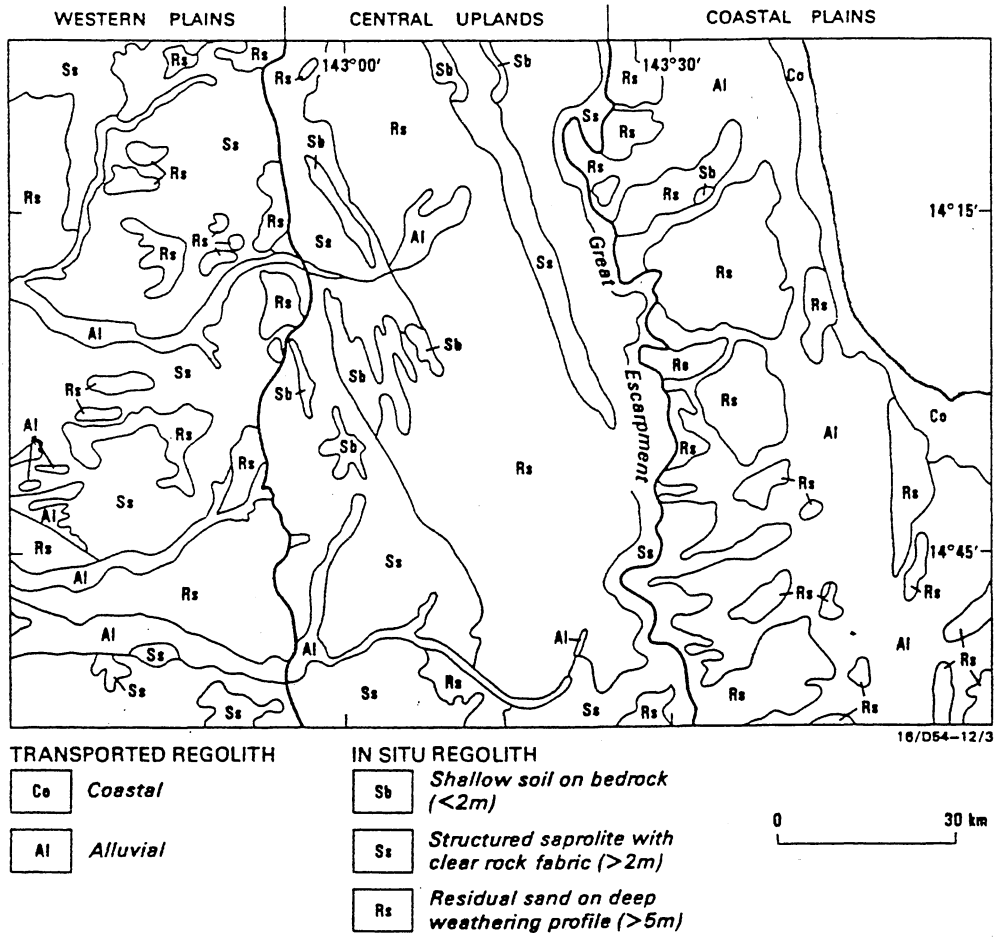


**Figure 5. Major regolith landform units over Ebagoola 1:250 000 sheet, including the western plains, central uplands and coastal plains. The distribution of in situ and transported material, and the location of the Great Escarpment is shown.**

Broad, extensive, braided river and alluvial fan deposits occupy much of the area between the Great Escarpment and the coast. They consist of channel sands and overbank sand, silt and clay. Soils are generally sandy, with uniform textured profiles. Gently undulating hilly terrain between the alluvial plains consist of red and yellow earths and uniform-textured sandy soils over weathered sandstones and schists.

## 4.2 The Central Uplands

The Central Uplands consists of undulating terrain 150–200m above sea level and is underlain by granitic and metamorphic rocks of the Coen Inlier. The eastern margin of the uplands is the edge of the Great Escarpment (Fig. 5 & 6). Landforms on granite are typified by low to moderate relief with highly weathered siliceous sandy soils and poorly exposed bedrock with outcrops typically confined to stream channels or as protruding granite tors and boulders. Landforms on metamorphic rocks are typified by steeper slopes and higher relief. Resistant quartzite strike ridges rise 160m above the surrounding landscape in places. Alluvial and colluvial sediments including cobbles and gravels form foot-slope deposits adjacent to steeper hills and ridges.

## 4.3 The Western Plains

The Western Plains are characterised by low relief and sandy red and yellow earths derived from *in situ* weathering of underlying sandstone and mudstone. The broad rivers (Coleman and

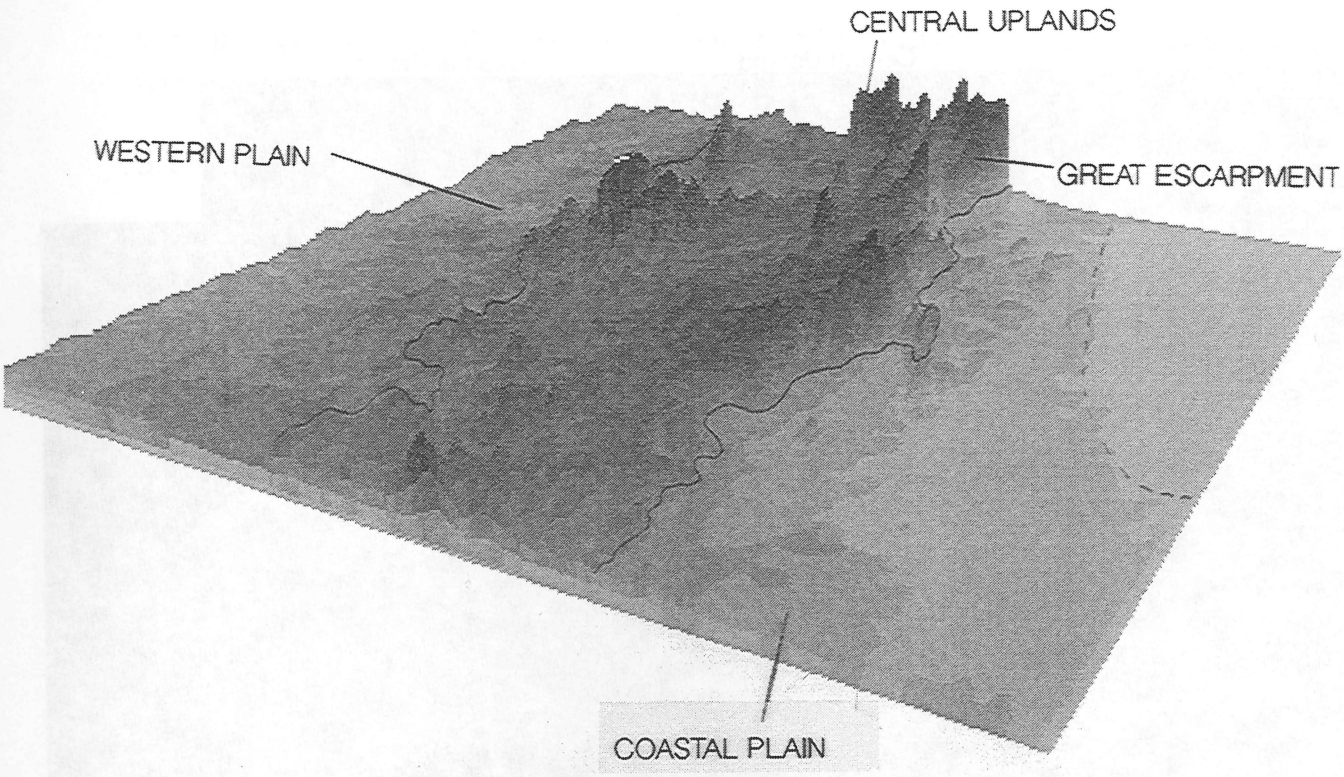


**Figure 6. Digital elevation model over the Ebagoola 1:250 000 map sheet as a perspective image viewed from the SSE. The model is based on 1km spot height data re-sampled to a 200m x 200m grid. The steep break in slope on the inland edge of the Coastal Plain corresponds to the east-facing Great Escarpment which separates the Coastal Plains to the east from the higher, undulating Central Uplands to the west.**

Holroyd) that traverse the plain are characterised by sandy channel and silty overbank deposits. Partially dissected plateau with highly leached pisolitic iron and bauxite soil profiles form remnant surfaces.

## 5 INTERPRETATION OF LANDSAT TM DATA

Landsat TM imagery contains attributes reflecting the type and distribution of surface materials and landform types. Surface materials can be discriminated and mapped on the basis of their spectral properties. TM landform characteristics, however, are a combination of variations in sun illumination caused by the topography and interactions between the vegetation and landform. One of the most effective ways to map landforms and structural elements on TM imagery is by using a single-band black and white (monochrome) image. This is because the high spatial component which includes landform and structural features is more readily detected by the human eye in monochrome than in colour (Drury, 1987).

The edge-enhanced image (Fig.7a) can be described in terms of four properties: tone, texture, pattern and shape. The tonal response is almost totally controlled by vegetation cover and areas of exposed rock and soil. Dark image tones are mainly vegetation (Landsat band 5 corresponds to water absorption in the shortwave infrared region and is highly sensitive to leaf water content); areas of exposed soil and rock appear as brighter tones. Siliceous sandy interfluves developed over granitic bedrock (center of the image Fig.7a) and silty alluvium associated with the braided river channels east of the Great Escarpment, appear bright in the image. The tonal response contains relatively little information for structural and landform interpretation, although

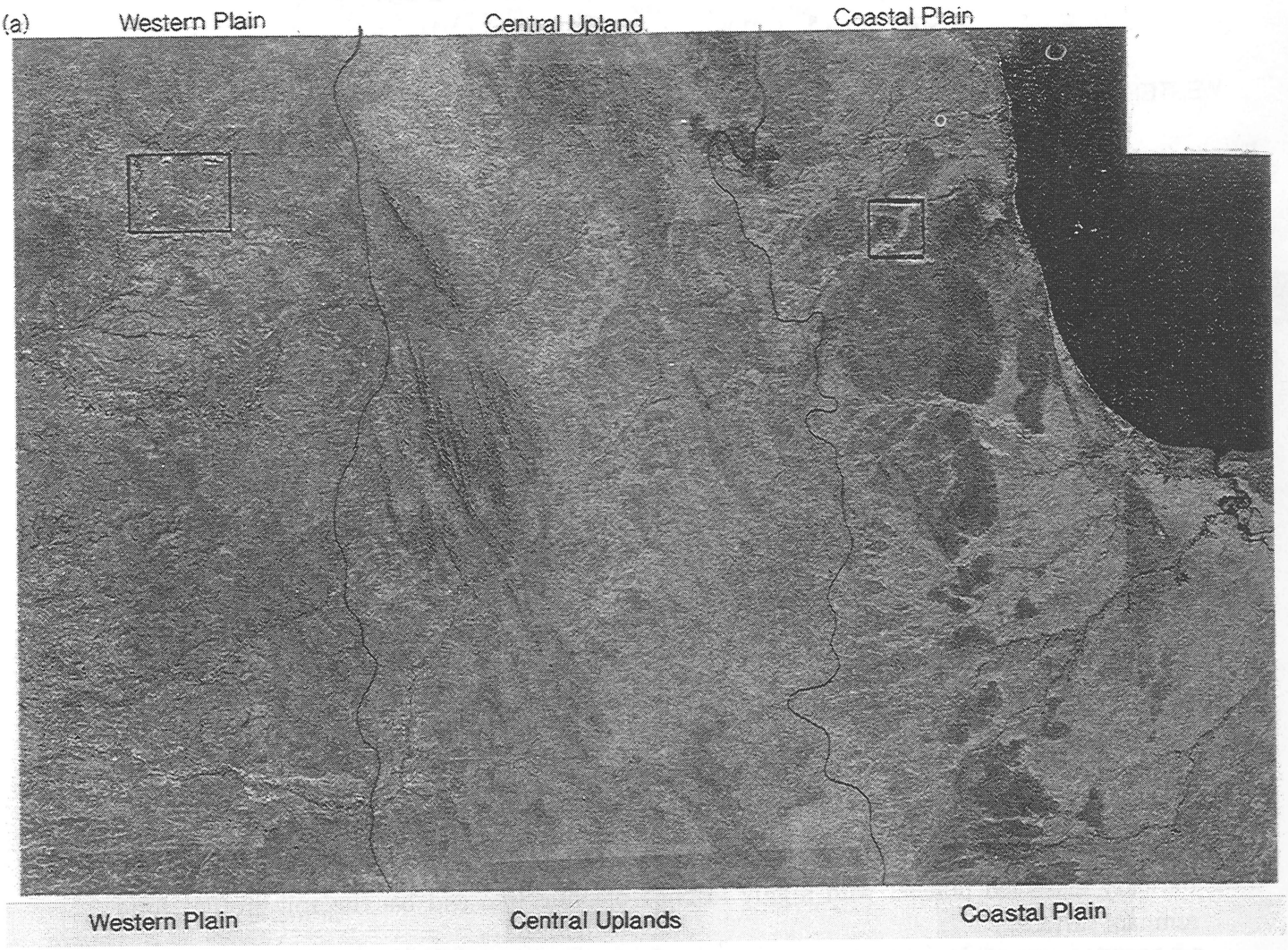


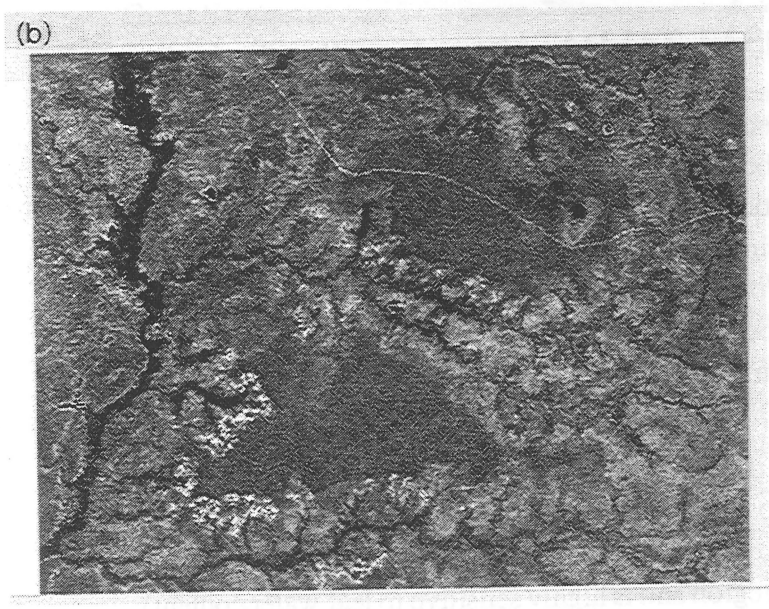


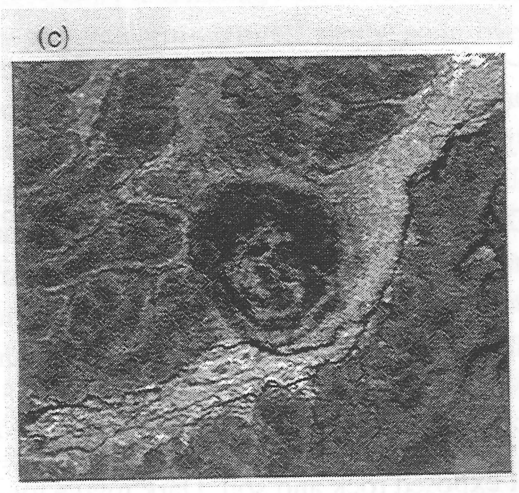


**Figure 7. (a) Edge-enhanced TM (band 5) image over Ebagoola. Considerable detail is lost in presenting the image at this scale, but it serves to highlight major geomorphological, regolith and vegetation characteristics of the region. Boxes indicate location of expanded views in Figures 7b and 7c. (b) Bauxitic plateau appear as darker tones, reflecting a dense tree canopy. (c) Circular remnant of a basalt plug is identified center of image.**

vegetation can be used indirectly to obtain information on landform type and properties of the regolith.

## 5.1 Hydro-botanical associations

Several hydro-botanical associations which indirectly provide information on the underlying regolith can be identified in the imagery. The availability of soil moisture is one of the main controlling factors governing the distribution of vegetation, and will vary locally in a region depending upon landscape position (i.e. areas of drainage *vs* collection) and the properties of the substrate including soil permeability and porosity. The response of vegetation to water availability is readily identified in the TM imagery, with healthy and dense vegetation appearing black in the imagery (Fig. 7a).

A hydro-botanical association can be used to distinguish old, residual, deeply weathered bauxitic plateau in parts of the Western Plains. The plateau appear on the imagery (Fig. 7b) in black to grey tones caused by dense vegetation, which consists of tall stands of bloodwood, stringybark and paperbark. The dense stands of eucalypts probably reflect the well-drained character of the soils and the availability of water contained within a near-surface kaolin aquifer throughout the dry season. Other gently undulating landforms with deep (60cm), sandy pisolitic soils derived from deep *in situ* weathering of siliceous Mesozoic and Tertiary sandstones also contain a permeable and porous substrate in which water can be stored. Soil moisture trapped within this layer is able to support a densely wooded vegetation cover which is characterised on the imagery by grey to black tones (Fig. 7b).

Shallow, isolated, circular or kidney-shaped depressions (commonly called melon holes) can be discriminated in the imagery by their haloes of dense vegetation. Doutch (1976) considered them to be a deflation feature formed during a period of desiccation, whilst Grimes (1979) interpreted them as laterite-karst depressions. Although many melon holes do appear to have formed by dissolution of material at the surface as a result of groundwater seepage, others appear to have formed from the breakdown of older drainage channels. Thus there may be several mechanisms by which these shallow depressions may have formed. Melon holes occur over much of the Ebagoola area, but are most common on the western plains. They appear to be associated with older parts of the landsurface and on the highest parts of interfluves. Other melon holes appear to be linked with older river channels particularly those melon holes on interfluves (usually appearing as disconnected strings), and can be used as an indicator of palaeodrainage lines.

## 5.2 Landform information

Pattern and textural elements of the image contain the greatest amount of landform information. These elements are most effectively enhanced by hillshading the image which sharpens lines associated with ridges and rivers (Fig. 8). The moderate to high-relief strike ridges of the folded and faulted Coen Metamorphic Group and Holroyd Group within the Coen Inlier are clearly delineated, and contrast with the gently undulating, low-relief, rounded interfluves associated with granitic landforms. Linear beach ridges and chenier plains parallel to sub-parallel to the coast (Fig. 5 unit Co) are also readily discriminated on the imagery (Fig. 9a).

The pattern and textural component can be used to map drainage patterns and density. Due to the overall low relief of the map sheet area, the apparent drainage channels seen on the imagery

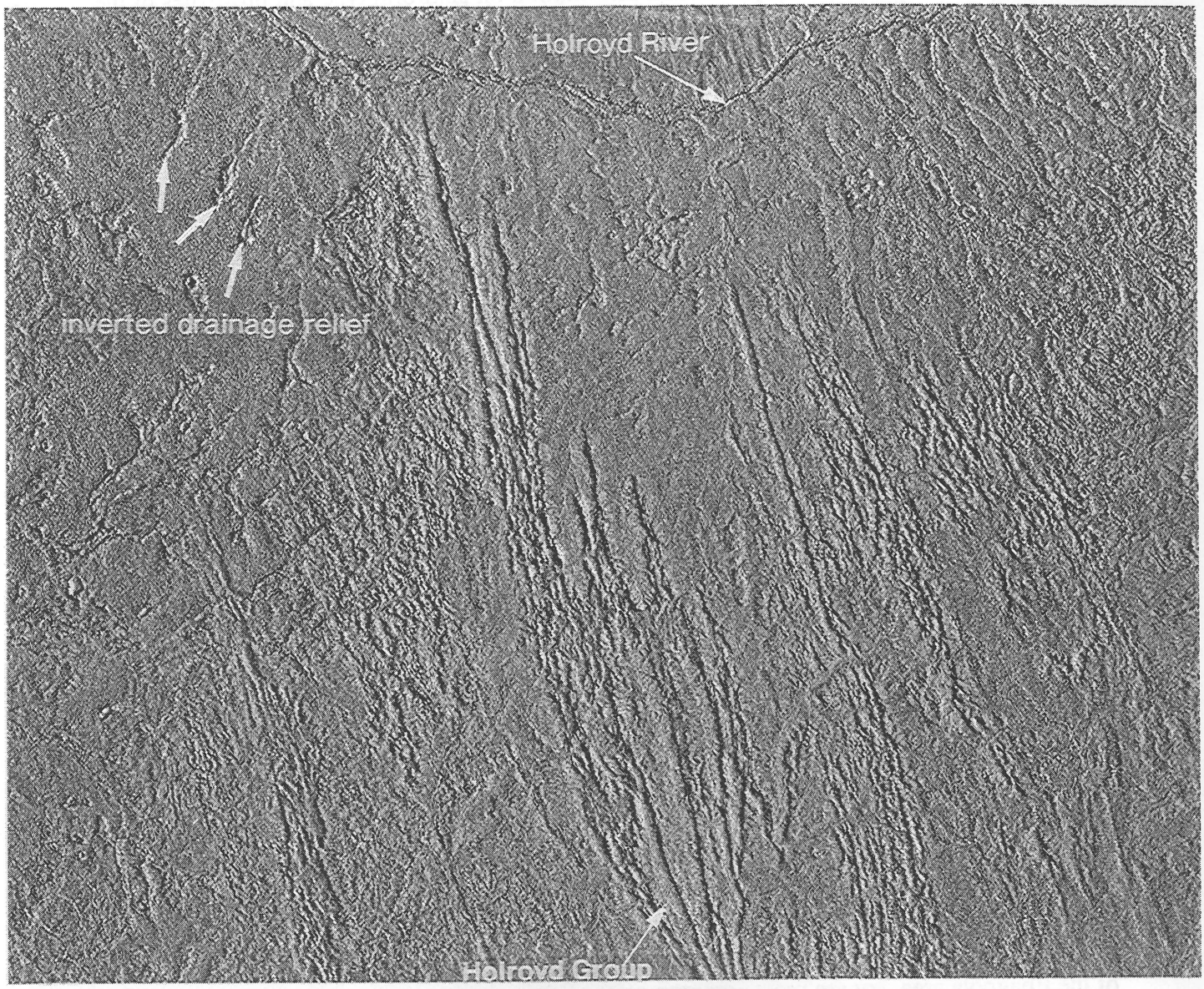


**Figure 8. Subset of a hillshaded (high-bandpass filtered) TM scene with east/west illumination, showing major landform and structural elements; including folded metamorphic rocks (Holroyd Group), river channels and inverted drainage relief (indicated by arrows).**

are edges of gallery forests along the rivers and streams rather than the shadow relief impressions caused by drainage incision. Drainage density variations within a local area are largely determined by the erodability or permeability of the bedrock. Anabranching, dendritic and distributary drainage patterns occur on the alluvial plains east of the Great Escarpment (Fig. 9a). Dendritic drainages are most common on the granitic terrains, although radial drainages associated with some individual plutons also occur. Variation in drainage density is one of the criteria which can be used to discriminate between different granites within the Coen Inlier. Recent mapping (Ewers & Bain, 1992) has identified muscovite-biotite granites, characterised by relatively widely-spaced dendritic drainage, and monzogranites to granodiorites characterised by relatively closely-spaced dendritic patterns. This variation reflects differences in the composition, texture and structural fabric of the granites. The granodiorites and monogranites have more closely-spaced jointing patterns, and appear to 'shed' their weathered products more readily than the muscovite-biotite granites. Drainage lines in the metamorphic

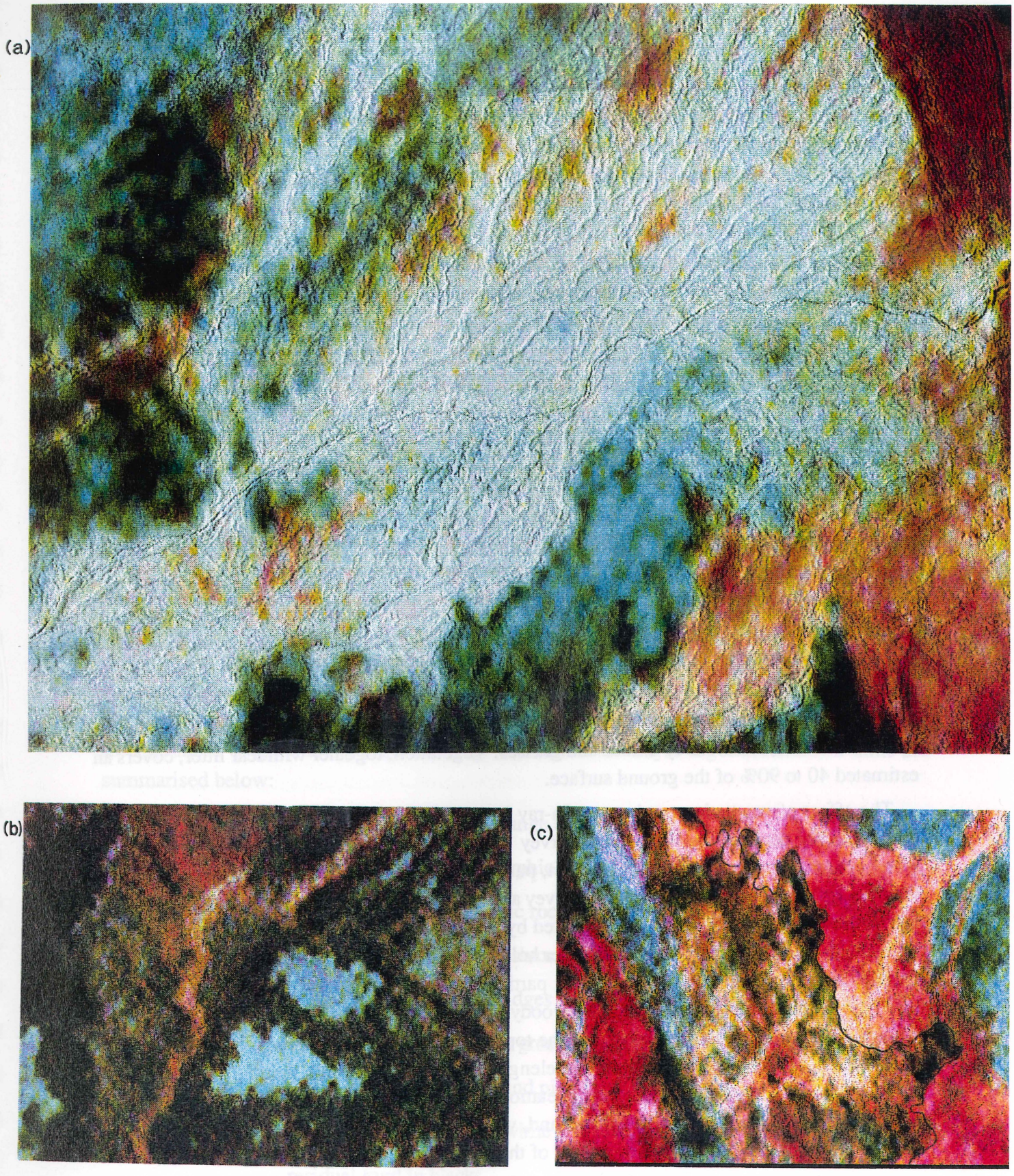


Figure 9. Combined Landsat TM and gamma-ray images (K,Th,U = RGB). (a) Northeast corner of Ebagoola 1:250 000 scale map sheet shows channel and overbank sediments of the Stewart River in white and linear beach ridges in reddish hues along the coastal fringe. (b) Bauxitic plateaus in light blue/green. Yellowish/reddish hues are associated with channel sands of Pretender Creek, reddish hues (high potassium) characterise areas of cracking clay soils and, black hues show areas of residual sand (50cm) over bedrock. (c) The edge of the Great Escarpment is defined by the contact of the older, stable, deeply weathered granitic landforms in green/black hues with the eroding slopes of the Escarpment (traced in black) in reddish hues.

belts are characterised by trellis patterns, reflecting the strong NNW foliation and cleavage development. Interrupted and widely spaced drainage channels occur on the highly weathered and porous bauxitic plateaus of the Western Plains, and on sandy and iron pisolitic soils developed on Mesozoic and Tertiary sandstones on the Coastal Plain. Drainage lines on Mesozoic sandstones and mudstones on the Western Plains are generally dendritic in form with low relief, gently undulating landforms, and rounded interfluves.

The shape component in the imagery gives evidence for specific landform types. The circular basaltic plug and broad alluvial fans on the Coastal Plain, and residual bauxitic plateaux of the Western Plains are examples (Fig. 7b & 7c).

## 6 COMPARISON OF GAMMA-RAY DATA WITH LANDSAT TM

Landsat imagery has been used with mixed success in mapping rocks and minerals based on their spectral properties over parts of the Australian continent. Several major obstacles need to be overcome, such as the effects of vegetation and fire-burn before the full potential of remote sensing for geoscience is realised in Australia (Simpson, 1990). Preliminary image processing (principal component analysis, ratios) of the Landsat TM imagery over the EBAGOOLA serves to highlight some of these obstacles.

Despite the spatial and spectral resolution of the Landsat TM data being higher than that of the gamma-ray survey data its effectiveness as a mapping tool is limited by the masking effect of vegetation on the characteristics of underlying rock types and soils. Firescars also have a confusing effect in distinguishing rock and soil boundaries on the TM imagery. The vegetation cover over the Ebagoola sheet area consists of eucalypt open-forests and woodlands, Melaleuca open woodlands, understorey shrubs and grasses. Vegetation, together with leaf litter, covers an estimated 40 to 90% of the ground surface.

The effect of vegetation on the gamma-ray imagery was very slight, even in areas of dense cover, mainly because the gamma-ray survey data were recorded during the dry season when water content of the soil and of vegetation, particularly perennial and annual grasses was low. Gamma-rays detectable by the airborne survey are emitted from the ground to a depth of 30–40cm below the surface. This depth was calculated by correlating gamma-ray values with thicknesses of residual sand cover measured from auger holes (Wilford, in prep). Gamma-rays are very high frequency electromagnetic radiation with particle like properties which are able to penetrate through several centimeters of leafy and woody material. In comparison the Landsat TM sensor records reflected radiation and measures the top few microns of the surface, with the exception of TM band 7 (10.4–12.6 micrometer wavelenghts) which records bulk thermal properties. The ability of gamma-rays to penetrate the vegetation cover and measure near-surface materials was extremely advantageous in north Queensland, where the terrain is highly vegetated and deeply weathered with sandy soils masking much of the underlying regolith or bedrock.

## 7 INTERPRETATION OF GAMMA-RAY DATA AND MERGED GAMMA-RAY/TM IMAGERY

Three representations of airborne gamma-ray spectrometric and TM data were assessed for their capacity to provide regolith/landform information. These were: a hillshaded additive three-band false-colour composite gamma-ray image (Fig.4a), a merged hillshaded Landsat TM and gamma-

ray image (Figs. 4b & 9a,b,c) and gamma-ray spectrometric profiles (Fig. 10). Comparison of these data sets with bedrock boundaries derived from the Ebagoola 1:250 000 scale geological map (Bain & others, 1992) showed a broad degree of correlation. However, variation within these major bedrock boundaries due mainly to the higher frequency component of the gamma-ray signal relates to regolith materials or more specifically soils, and geomorphic features in the landscape (Fig. 10).

The gamma-ray data relate mainly to the presence and distribution of radioactive elements in the soil cover, or in bedrock where it is exposed at the surface. Soils form the uppermost layer of the regolith. Whereas most soil maps are based on the physical and chemical properties of the soil profile to a depth of up to 150 cm; regolith, which extends to fresh unweathered rock, may be tens of metres in depth. Discrimination between soil types can be used to map the regolith directly where soils overlie bedrock, or indirectly where soils are diagnostic of deeper regolith profiles. Where bedrock is exposed in outcrop, the gamma-ray response can be directly related to lithology. The gamma-ray response over areas of thin *in situ* weathered regolith correlate well with bedrock chemistry (Fig. 10).

The imaged gamma-ray data sets displayed as potassium (red), thorium (green) and uranium (blue) ( Figs.4a,b; 9a,b,c & 16b) effectively mapped bedrock geology and different soil types over variable landforms and vegetation covers. The imagery discriminated between areas of *in situ* weathered and transported material in the landscape, different styles of weathering, surfaces of different ages, areas of active erosion and transportation (areas of high process rates), and major morphotectonic features. The three broad regolith-landform units, Coastal Plain, Central Uplands and the Western Plain, are clearly depicted on the gamma-ray image (Fig. 4a). Interpretation of gamma-ray response (Fig. 4a) within the major regolith-landform units are summarised below:

| | |
|---|---|
| Coastal Plain | –alluvial fans in reddish/orange and white hues |
| | –*in situ* weathered metamorphic rocks in greenish/blue hues |
| | –*in situ* weathered Mesozoic rocks in black |
| | –coastal sediments in reddish/orange |
| | –young and older coastal ridges in reddish and black hues, respectively; |
| Central Uplands | –*in situ* metamorphic rocks greenish/white hues |
| | –*in situ* granitic rocks red and pink hues |
| | –channel alluvium in red, white and blue/green hues |
| | –residual sand in black; |
| Western Plain | –residual sand in black hues |
| | –*in situ* weathered rock in greenish hues |
| | –channel alluvium in white and pink hues |
| | –bauxitic soils in greenish/blue hues. |

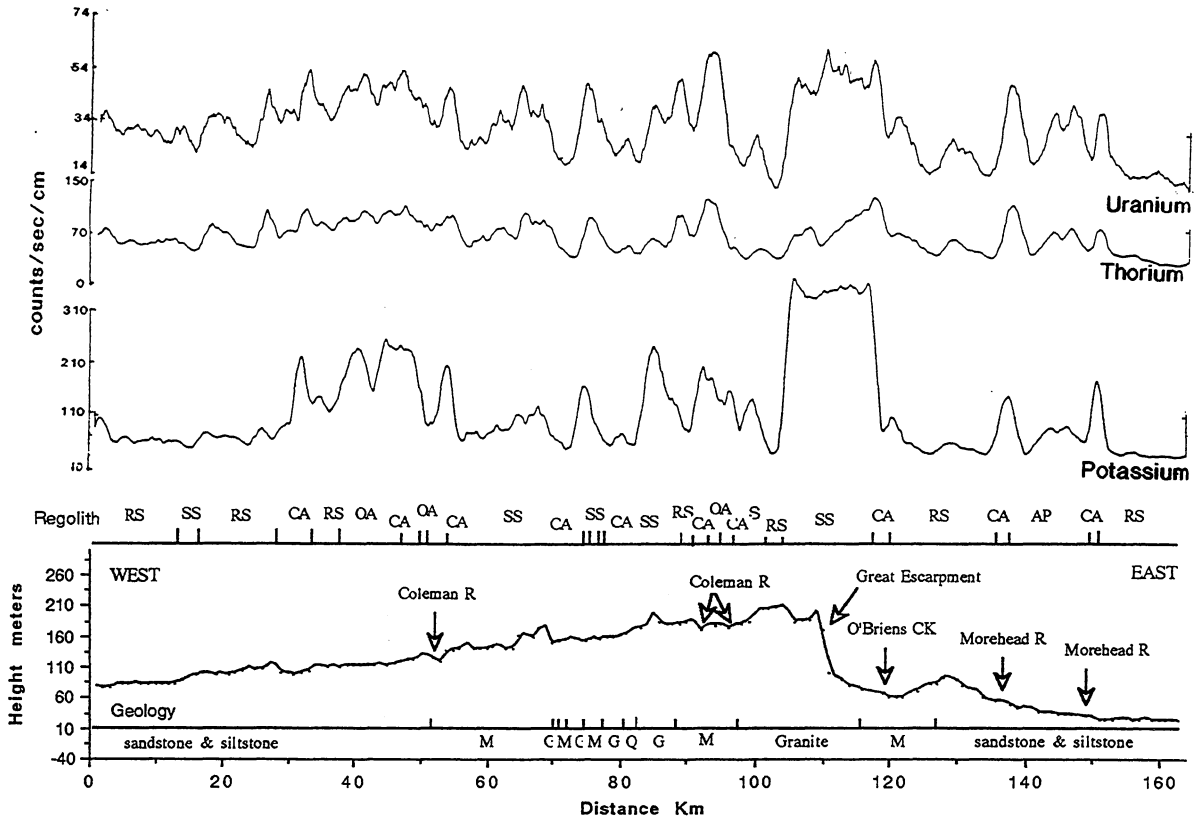


Regolith RS=residual sand, S=saprolite, SS=structured saprolite, CA=channel alluvium, OA=overbank alluvium & AP=alluvial plain.

Bedrock G=granite M=metamorphic & Q=quartzite

**Figure 10. Gamma-ray spectrometric profiles of potassium, thorium and uranium compared with the topographic profile and simplified regolith and bedrock geological boundaries. Although a broad correlation exists between the gamma-ray response and the underlying bedrock, most of the higher-frequency variation in the gamma-ray profiles corresponds to variation in regolith materials and morphotectonic features in the landscape. High gamma-ray responses over areas of recent river alluvium reflect its bedrock provenance of the alluvium. Similar responses from in situ weathered rock correlate well with bedrock chemistry. Low responses correlate with areas of residual sand. These sands form the top of deeply weathered regolith profiles. Removal of the residual sand cover over granite associated with the Great Escarpment is clearly defined by the very high potassium response.**

# 8 REGOLITH Discrimination

## 8.1 Coastal Plain

Geomorphic processes on the coastal plain are characterised by mechanical transportation and deposition of sediments derived from metamorphic and granitic rocks of the Central Uplands. These sediments are deposited as broad alluvial outwash fans and braided stream deposits, or are reworked by tidal and wave action into beach ridges and chenier plains along the coastline. The rocks shedding the sediment can be readily distinguished in the imagery. Red and orange hues indicate high potassium which correspond to mica and K-feldspar in sediments derived from weathered granite. Blue/green hues indicating relatively high uranium and thorium which probably correspond to heavy minerals such as zircon, titanite, sphene and monazite (Table 1), are seen in sediments derived from weathered metamorphic rocks. Mixed sediments derived from granite and metamorphic rocks are depicted on the imagery in white hues indicating high

potassium, thorium and uranium values. Braided river channel and fan deposits of the Stewart River (Fig. 9a) are a example of alluvial sediments derived from granite and metamorphic rocks. Loamy and silty solodic, grey clay, sandy red, and yellow earth soils have developed on overbank and channel sediments which form broad outwash fans and alluvial plains. These soils contain mica and minor K-feldspar which correspond to reddish image hues (i.e. high potassium).

Various coastal sediments can be resolved in the imagery. Beach ridge sands have virtually no gamma-ray response and appear black in the image. This is because the more unstable radioactive element-rich constituents such as K-feldspar and micas have been removed. A thin black line on the central eastern side of the imagery, sub-parallel to Princess Charlotte Bay (Fig. 4a) corresponds to an older beach strand-line up to 15km inland from the present coast. This strand-line is probably coeval with Pleistocene beach ridges along the west of Cape York Peninsula (Smart, 1976). Younger (Holocene) beach-ridge sands consisting of quartz, minor mica and shelly material appear in pinkish hues due to the potassium in mica. Dark grey to brown, cracking clay and saline soils associated with coastal and estuarine sediments (silts and clays) of Princess Charlotte Bay appear in pink hues. This is probably due to potassium in mica and minor feldspar in sediments derived from weathering of granites further inland. The high potassium response may be also partly due to potassium salts present in supratidal sediments and hypersaline deposits in saltpans.

Chenier plains consisting of long sandy ridges sub-parallel to the coast appear in reddish hues (Fig. 4a) indicating relatively high potassium content, and probably also reflecting the presence of mica and minor feldspar. An abrupt change in the gamma-ray response between the alluvial sediments along the Stewart River (bright white) and sediments distributed along the coast north and south of the river mouth (red-brown hues) can be seen top right of the image (Fig. 9). If the coastal sediments originate from the Stewart River, this change may be due to the winnowing out of heavy minerals by tidal and wave action, resulting in a relative increase in potassium over thorium and uranium. Alternatively, it may be a result of longshore drift from the south of coastal sands with different mineralogical composition.

Bedrock exposure in the coastal plains is poor because of the extensive transported cover, which effectively blankets underlying lithologies in the area. However, deep, sandy red and yellow earth soils developed on Mesozoic and Tertiary sandstones on the Coastal Plain are resolved in the imagery (in black) and can be separated from adjacent shallow sandy soils (greenish/blue–Fig. 4a) over metamorphic rocks. Soils over the Mesozoic and Tertiary sandstones on the imagery (Fig. 4a) appear black because of the abundance of quartz. Soils over metamorphic rocks appear in green/blue tones from the high thorium and uranium values which probably relate to the presence of accessory minerals such as monazite, zircon, and titanite (Table 1) in the profile.

## 8.2 The Central Uplands

The central uplands is essentially an erosional landform, and its regolith is dominated by *in situ* weathered bedrock. Weathered material is removed from the uplands by both physical and chemical means: removal of material in solution, and mechanically in the clay and silt fraction are probably the most important processes volumetrically as is evident from the thick accumulations of residual quartz sands on granite landforms. Two main regolith landform

associations are distinguished on the imagery; landforms with moderate to high relief on metamorphic rock, and granitic landforms with low relief.

### 8.2.1 Landforms on metamorphic rocks

The metamorphic rocks are weathering to various degrees reflecting their lithological heterogeneity. Steep NNW-trending quartzite ridges alternate with valleys and belts of undulating country underlain by weathered schists, phyllites and grainte. Scree and lithosols on quartzite ridges appear in pale blue tones because of the heavy mineral content (i.e zircons) of the quartzites (Fig. 4b). Regolith is characterised by shallow lithosols overlying weathered bedrock and as a consequence the gamma-ray response is highly correlated with bedrock composition.

The regolith along valley floors and over gently undulating landforms underlain by schist, phyllite and gneiss bedrock consists of red and yellow sandy earths and red podozolic soils. Soils over schist and gneiss appear black to reddish-green probably because of their sandy texture and mica content, podzolic soils and earths vary in response from black to reddish green. The sandy soils developed on phyllites correspond to black and dark blue image tones. Rich red burgundy sandy earths over greenstones are low in potassium, thorium and uranium, and appear in black/dark green hues on the imagery.

Cainozoic sediments (characterised by black to dark blue image tones), including footslope deposits, pediments and colluvial fans, consist of poorly sorted sand, gravel and cobbles. Proximal footslopes commonly contain quartzitic boulders in a coarse gravel and sand matrix. Many of these deposits have been cemented to various degrees by iron, to form mottled ferriuginous duricrusts up to 7m thick. In many places on the imagery, it is difficult to separate weathered phyllite and schist bedrock from these Cainozoic sediments. Quaternary sediments comprise of alluvial sands and gravels typically mottled at depth, and partially indurated in places by ferriginous cements. Induration occurs adjacent to stream channels, and forms small blocky cliffs of alluvial hardpan. These deposits are in most cases too small to be easily distinguished on the imagery.

### 8.2.2 Granitic Landforms

The gamma-ray response over granitic landforms corresponds to plutons of different composition, soils, and geomorphic processes (discrimination between granite plutons using the gamma-ray imagery is discussed in Ewers and Bain, 1992). Granites weather more uniformly, (reflecting their relative mineralogical homogeneity) to extensive, gently undulating landforms with low relief. Regolith development on granitic landforms is typified by thick accumulation of residual quartzose sands. These sands form yellow to yellowish-orange massive earths and podzolic soils (typically with a bleached A2 horizon) which form the top of a deeply weathered uniform sandy textured profile which grade into saprolite and then granite at depth (Fig. 11). The depth of the weathering profile is variable, but probably extends as much as tens of metres below the surface. The sandy soils may be several metres thick on older more stable landforms – which have been subjected to deep *in situ* chemical weathering, where the more unstable soluble constituents (e.g. feldspars, mica) have been broken down and leached from the weathering profile, leaving behind residual quartz sand. Kaolinite is the dominant clay mineral in the soil, and forms coatings around the skeletal quartz grains.

The distribution of most regolith types over granite landforms are associated with a recurring

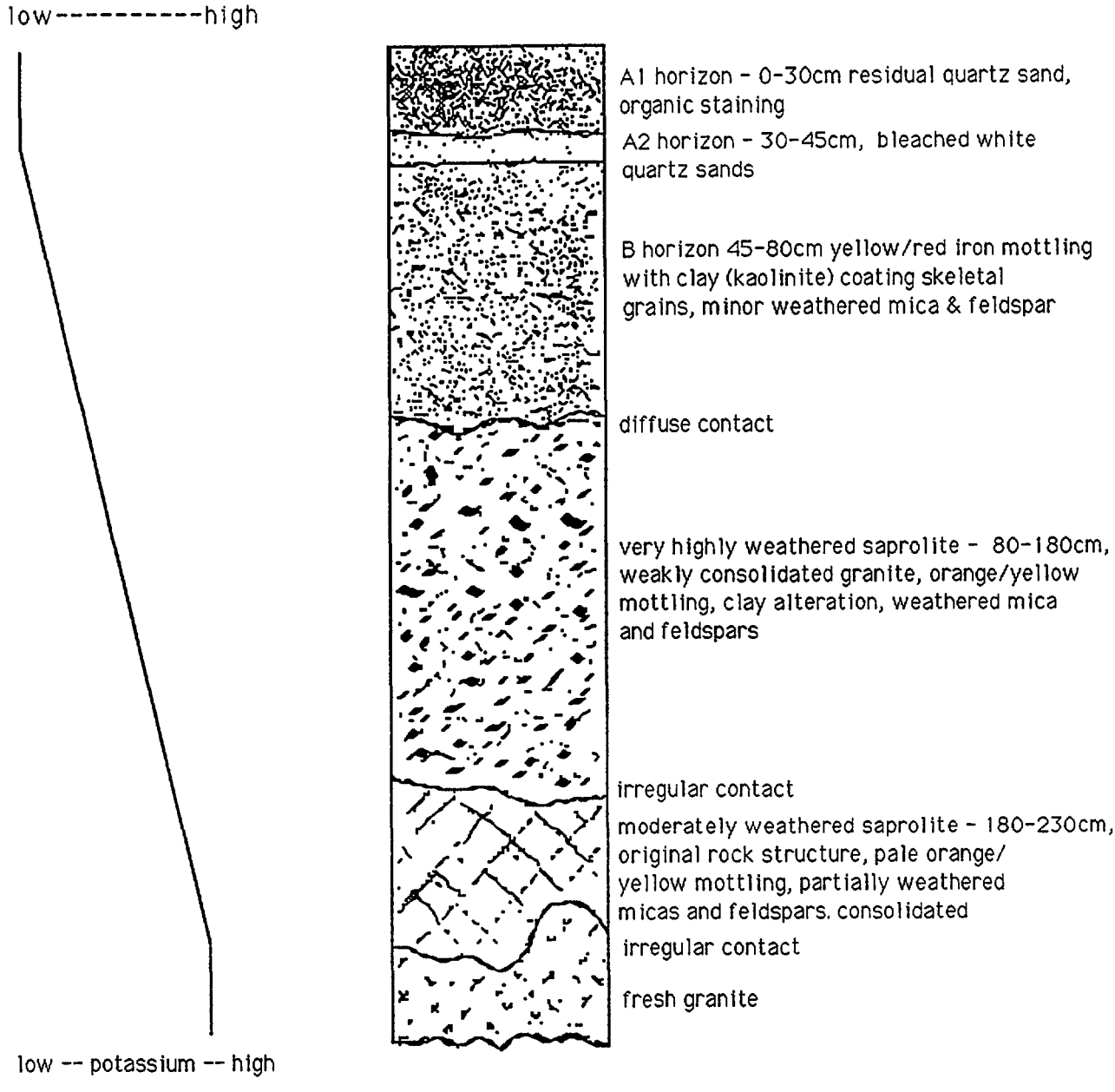


**Figure 11. Typical weathering profile on granite. Thicknesses of soil horizons will vary according to position in the landscape (see Fig.12). Refer to text for description. Left of the profile is an approximate guide to potassium abundance through the weathering profile. The potassium content increases down the profile from very low values, corresponding to surface residual quartz sands, to high values relating to mica and feldspar in the granitic bedrock.**

regolith toposequence consisting of soils ranging from deep sandy pale earths on ridge crests to shallow pale yellow podzolic soils and exposed structured saprolite on steeper gradients down slope (Fig. 12). This toposequence is identified in the gamma-ray imagery (Fig. 4a) with sandy earths appearing in black to greenish-black hues indicating the presence of quartz and heavy minerals (such as zircons) which may have been preferentially concentrated during weathering. Shallower, less mature soils on steeper slopes more closely approximate the composition of the bedrock lithology; they appear as orange-red hues (high potassium) in the image. Sandy soils mapped and analysed by Isbell & Gillman, (1973) over granites within the uplands show them to be very low in organic carbon, nitrogen, potassium, sulphur, phosphorus, copper, zinc and exchangeable cations. These low-nutrient soils correlate closely with the older, deeply leached sandy profiles appearing on the imagery in black and blue/green hues.

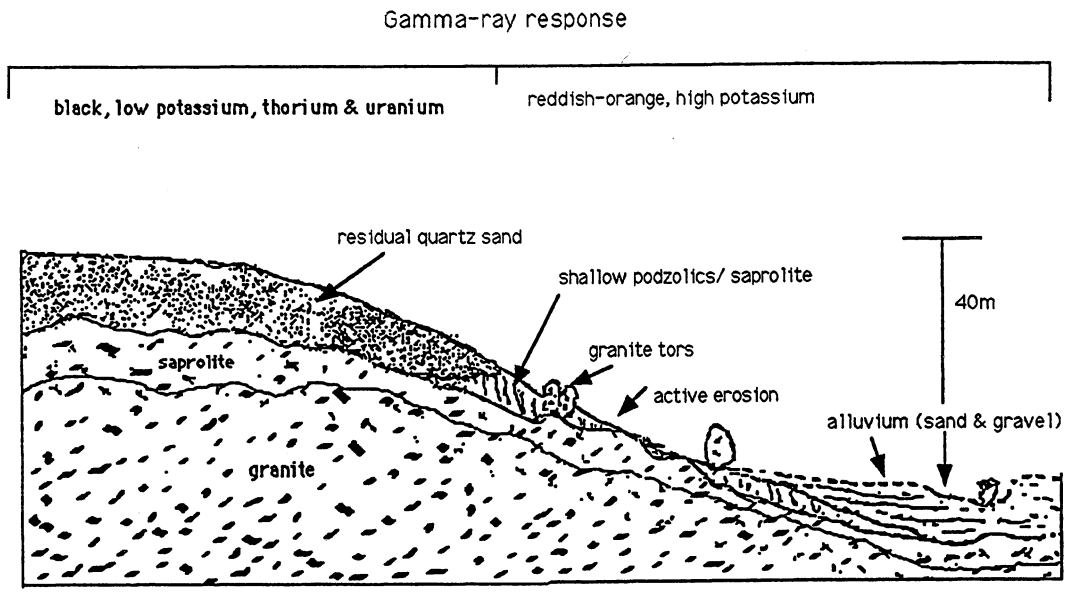


**Figure 12. Regolith toposequence over granitic landforms. Low hills are characterised by deep sandy earths. Down slope from these hills the soils and regolith are characterised by shallow podzolic and moderately weathered saprolite. The gamma-ray data is able to distinguish these different soil types with low gamma-ray (K,Th &U) responses typifying the sandy red earths and high potassium values typifying the podzolic soils and saprolite.**

## 8.3 Western Plains

The region is characterised by sandy soils over moderately weathered bedrock. Soils include sandy yellow earths and minor red earths over extensive flat to gently undulating landforms; solodic and bleached grey earths occur in drainage depressions and melon holes. On the gamma-ray images the red and yellow sandy earths appear in shades of black to greenish blue, because of the low gamma-ray values over areas of residual sand cover. The thorium/uranium response over these areas may correlate with heavy minerals such as zircon in the weathering profile.

Potassium values over the western plains are generally low except for alluvium associated with major rivers, and gently undulating landforms of cracking clay soils with gilgai micro-relief (top left side of Fig. 4a). High potassium in the alluvium is probably due to relatively high feldspathic and mica content of sands derived from the rocks of the Central Uplands. Brown clay to loamy gilgai soils are scattered over the plains, but are particularly well developed towards the northwestern corner of the Sheet area. These soils are distinguished by reddish orange hues (Fig. 9b). The potassium signatures associated with the cracking clays may indicate either the presence of potassic clays (e.g. illite) and/or absorption of potassium ions within the lattice of swelling clays (ie montmorillonite). Alluvial soils readily identified on the imagery (Fig. 4a &

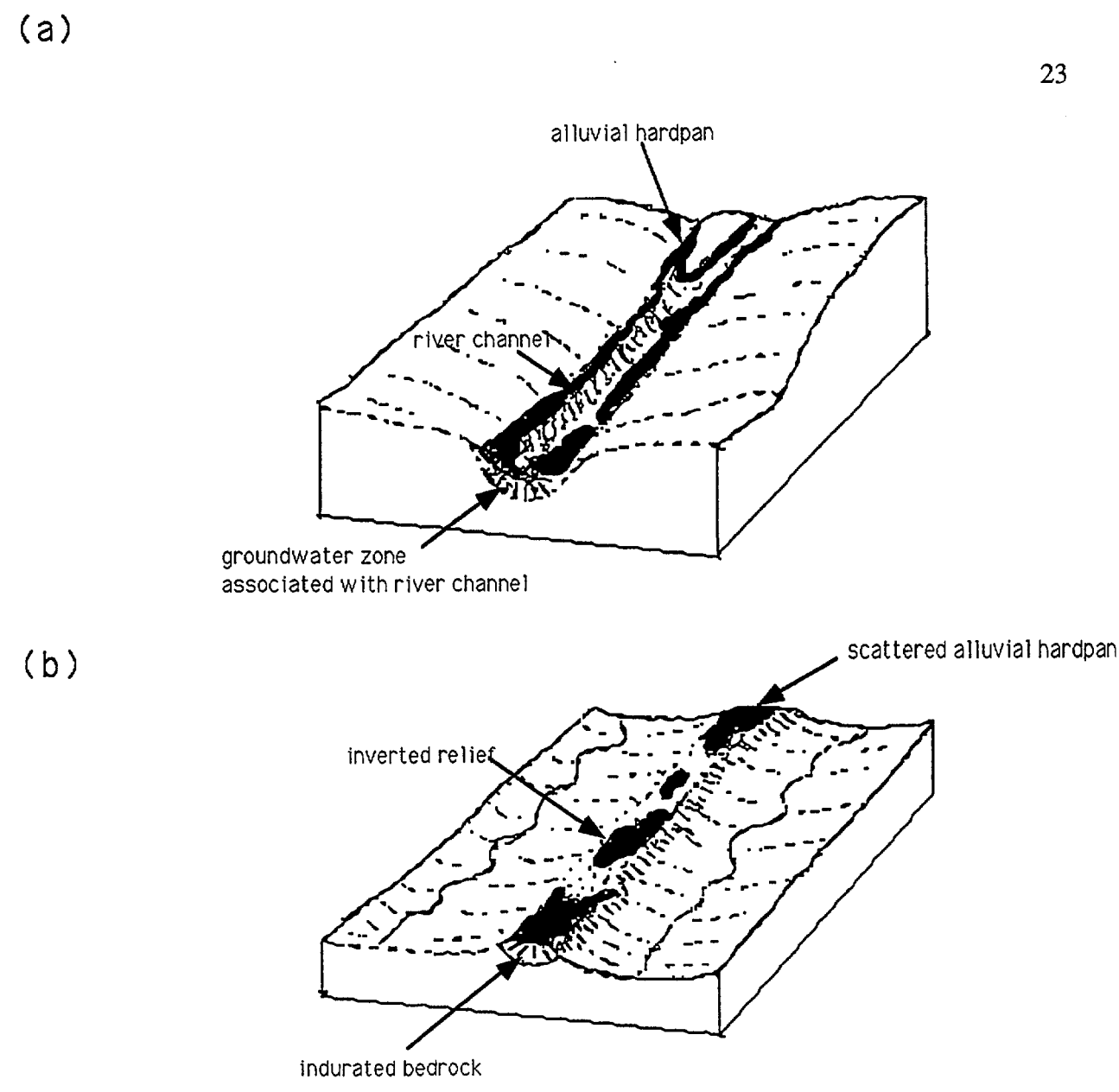


**Figure 13. Inversion of relief. a) Induration of sediments along the channel edge and bedrock immediately beneath the river by silica cements and/or iron-rich groundwaters leads to, b) relief inversion caused by differential erosion.**

16b), have developed on channel and overbank deposits and consist of deep red, brown and yellow sandy earths. Channel sands are recognised by their high K-feldspar content which produces reddish hues, as distinct from the green hues of soils developed on overbank sediments. The difference in image response between the two alluvial soils is probably due to variations in texture, overbank sediments being generally finer, and mineralogy, the channel deposits containing a higher proportion of K-feldspar (high potassium response). In addition, the overbank sediments are likely to be older and generally more weathered and leached: this would result in the less stable mineral constituents such as feldspar being removed, effectively concentrating more stable heavy minerals (e.g. zircons) in the weathering profile.

### 8.3.1 Relief inversion

Bedrock indurated by siliceous and ferriginous cements locally forms low ridges and residual hills. Many of these rises correspond to areas of relief inversion, where silica and iron-rich groundwaters have indurated regolith in the original valley floors. Differential erosion resulting from hardening due to induration eventually forms positive relief features from what was once a topographically low valley floor. This results in inverted relief (Pain & Wilford, in prep.) (Fig.

13). Some areas of inverted relief can be discriminated on the imagery: an irregular resistant plateau (40m local relief from surrounding plain) characterised by greenish blue hues (Fig. 4a) corresponds to a region of drainage inversion. The area consists of silicified mudstone and siltstone of the Rolling Downs Group forming a porcellanite capping several meters thick. Scattered quartzite gravels and cobbles on the porcellanite indicate that area was once a river valley. The greenish/blue hues indicating relatively high thorium/uranium to potassium values, probably indicate the presence of heavy minerals such as zircon in the porcellanite.

### 8.3.2 Bauxitic plateau

The blue-greens (high uranium and thorium) over low residual plateau correspond to highly weathered, ferruginous and bauxitic pisolitic profiles (Fig. 9b). The bauxitic profiles in the Ebagoola area are thinner and of poorer grade than their Weipa equivalents, consisting of a residual sandy (quartz) A' horizon (10-70cm), a bauxitic and iron – unconsolidated pisolitic zone with a sandy matrix (1.2+m) and a pallid zone consisting mainly of kaolinitic clay. The bauxitic profiles result from intense leaching and chemical weathering, and are similar in mineralogy to bauxites at Weipa, which consist of gibbsite and bohemite with small amounts of kaolinite and quartz. The main heavy minerals associated with these bauxites include zircon, leucoxene, rutile and tourmaline. Other minor grains include ilmenite, anatase, titanite, siderite, magnetite, apatite, monazite, andalusite, spinel and staurolite (Schaap, 1990). The high uranium and thorium counts are probably the result of preferential enrichment in the profile of some of these heavy minerals.

## 9 MORPHOTECTONIC FEATURES

Morphotectonic studies are concerned with the effects of tectonism on the morphology of landscapes. Several morphotectonic features which have a controlling influence on the distribution and type of regolith can be distinguished on the imagery. They include the Great Escarpment and faulting over parts of the Western Plains and Coastal Plains. Some effects of these morphotectonic features on weathering and geomorphic activity can been seen on the gamma-ray imagery.

## 9.1 The Great Escarpment

The Great Escarpment (Ollier, 1982), is an east-facing actively retreating landform separating the Central Uplands from the Coastal Plains. It trends almost parallel to the northeast coast of EBAGOOLA with steep to occasionally precipitous slopes, and local relief of up to 300m. It lies to the east of the Great Divide, although the two coincide in places. The edge of the Great Escarpment, clearly visible on the processed imagery (Figs. 4a, 9c & 16b) separates two different regolith-landform associations. First, deeply weathered residual sands (low potassium, thorium and uranium values) over gently undulating granitic terrain west of the Escarpment edge. Second, steep, actively eroding terrain east of the Escarpment edge where the residual sands and friable saprolitic layer have been partially stripped to expose relatively fresh granite (shown in the imagery by high potassium values).

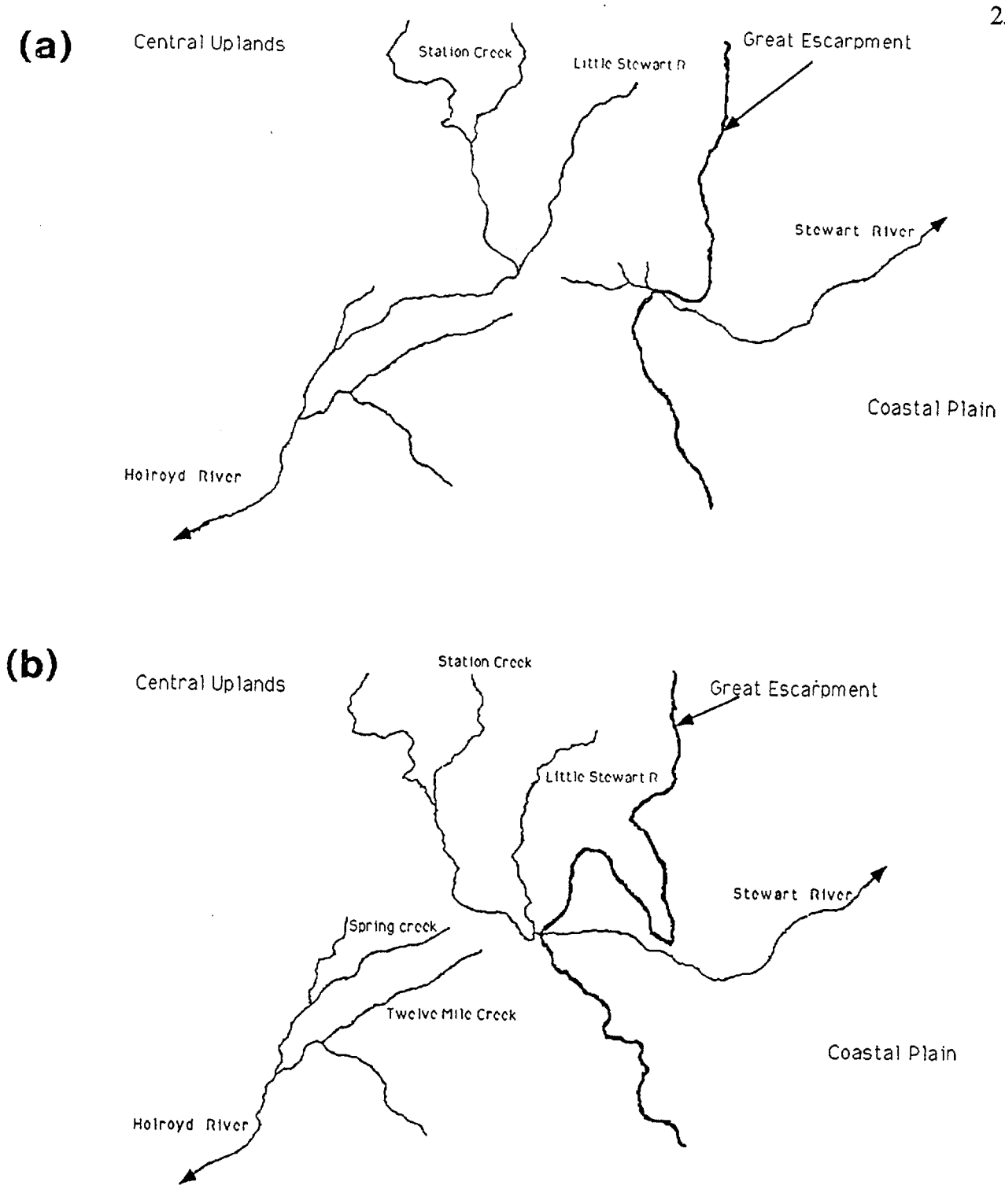


**Figure 14. (a) Before capture, the headwater channels (Little Stewart River and Station Creek) of the Holroyd River flowed into the Gulf of Carpentaria. (b) Progressive scarp and Knickpoint retreat captured and diverted headwater streams of the Little Stewart River and Station Creek to the east. The beheaded stream (Twelve Mile Creek), has reduced water volume, whilst the flow of Stewart River was increased by the additional volume of the Little Stewart River and Station Creek. A lower river base level was established, resulting in rapid downcutting and migration of the knickpoint up stream. This triggered active erosion within the immediate catchment area towards the new and lower base level.**

## 9.2 River capture

In places, as the Great Escarpment retreated westwards, some headwater streams of rivers previously flowing to the west were captured and their flow diverted to the east. An excellent example of this is the capture by Stewart River of the headwater streams of the Holroyd River (Fig. 14). Knickpoint retreat following river capture led to steeper gradients, rapid downcutting

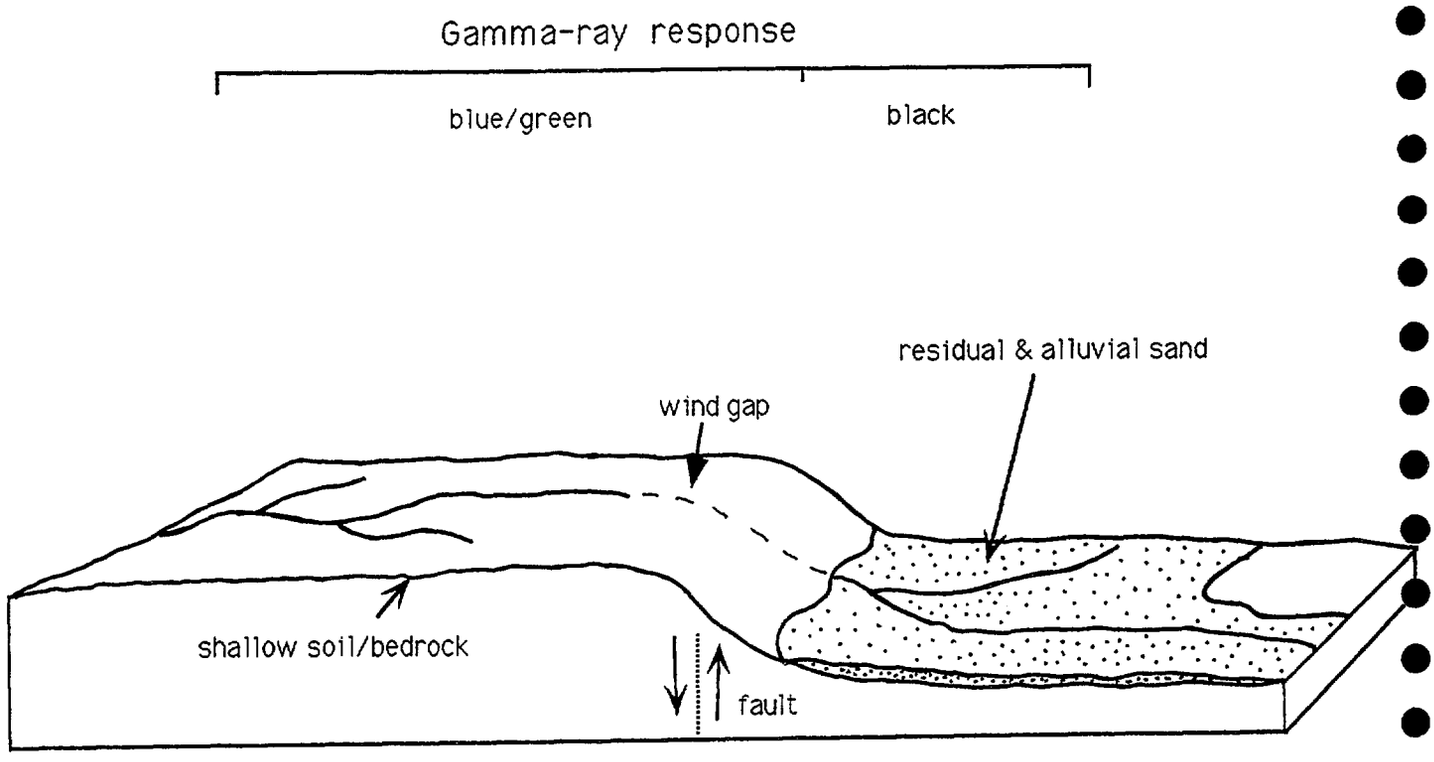


**Figure 15. Effect of faulting on drainage systems and sedimentation; the gamma-ray image response is indicated.**

and stripping of the friable saprolitic and residual sandy layer, and exposure of relatively fresh granite. The lower base level also initiated active erosion and stripping of residual sand on slopes within the immediate catchment area. This area of stripping is characterised on the imagery by very high total gamma-ray values (very bright colours/white) corresponding to relatively thin regolith cover over granite (Fig. 4a – top center).

## 9.3 Faulting

Movement along the NNW-trending Palmerville Fault adjacent to Princess Charlotte Bay (Fig. 1 and lower right corner of Fig. 16a) is probably related with gentle uplift and/or tilting of alluvial sediments immediately to its east. Streams have been diverted northwards around the area of uplift, except for Saltwater Creek where channel down cutting was sufficient to keep pace with uplift. Deep soil profiles have formed on the uplifted alluvial sediments; these contrast with the surrounding depositional plain, which is underlain by more recent channel and overbank sands and silt. The soil profiles are characterised by *in situ* chemical weathering and leaching which have led to the development of a deep residual sandy A' horizon. The underlying B' horizon consists of an iron-rich pisolitic and mottled zone formed by the vertical and horizontal movement of iron oxides, and fluctuating water tables within the zone. Because quartz sand has a low response in all three gamma-ray channels, these deeply weathered profiles appear black in the image.

Evidence of the effects of faulting on drainage and distribution of sediments on the Western Plains can be distinguished on the gamma-ray TM merged image. Faulting has beheaded and redirected some westward-flowing streams; this has resulted in the accumulation of alluvial sediments immediately behind the area of uplift (shown diagrammatically in Fig. 15). These sediments are characterised in the gamma-ray imagery (center left of Fig. 16a) by low gamma-ray

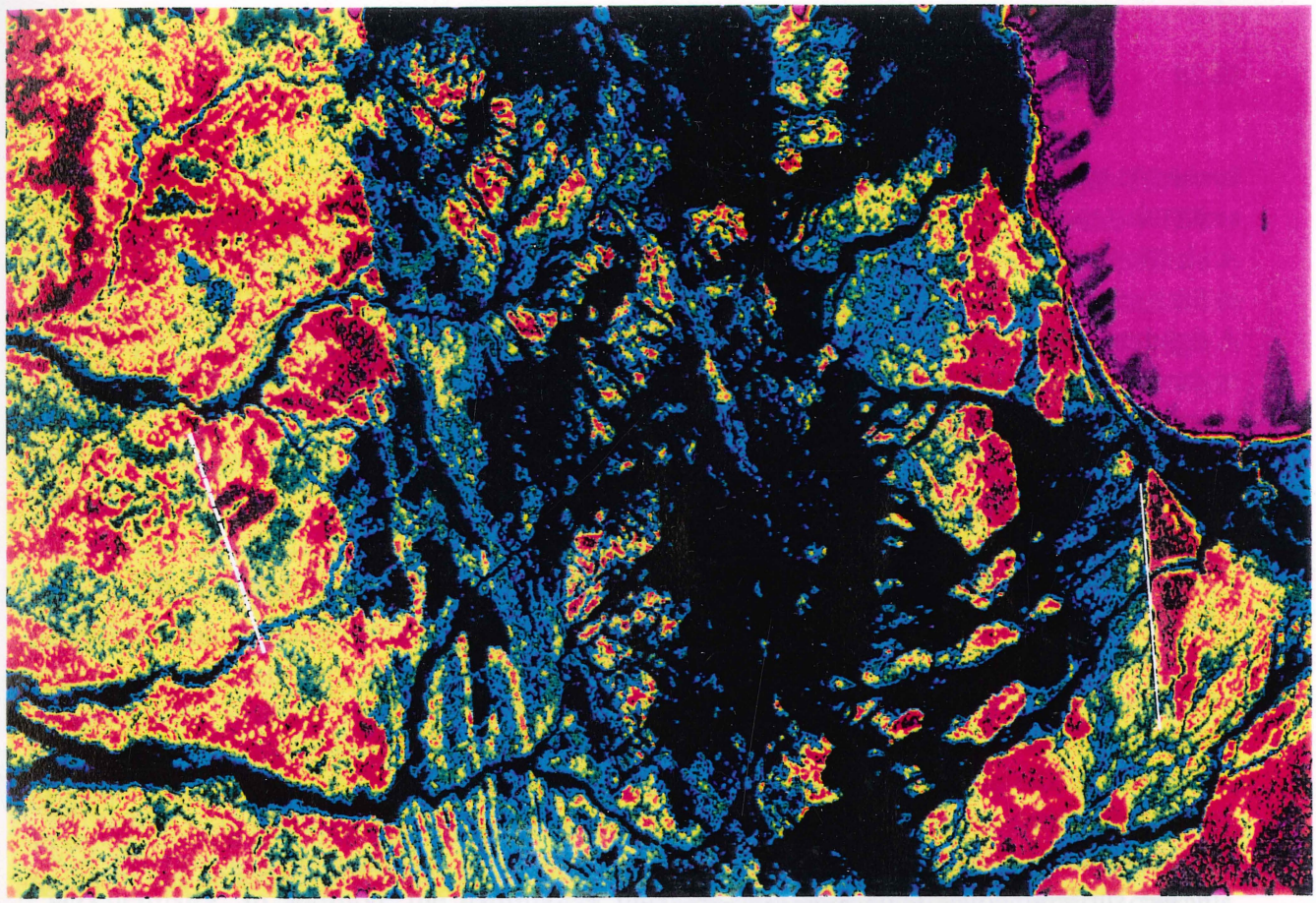

(a

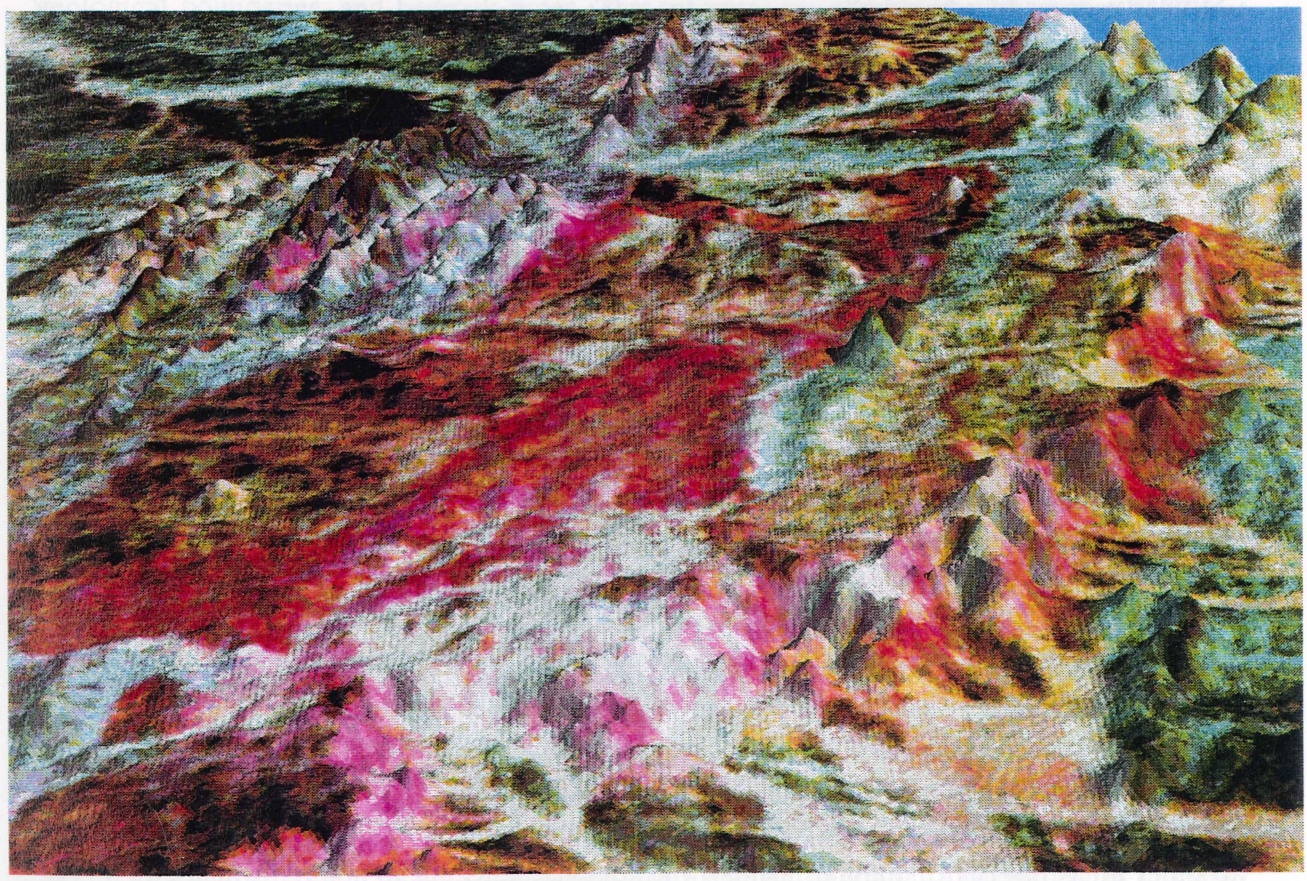

(b

Figure 16. (a) Pseudocolour gamma-ray image which has been processed to show the distribution of residual sands at the top of well-leached regolith profiles. The image is scaled from red through to blues and black. Reds and yellows map the distribution of residual sand, blue and black highlight areas of alluvium and relatively thin regolith over bedrock. The Palmerville Fault and NNW-faulting are shown by solid and dashed lines, respectively (see text for description) (b) Three-band gamma-ray image has been draped over digital elevation model to create a three dimensional perspective view. Eroding granites (in red) along the Great Escarpment which divides the coastal plains from the central uplands, are clearly displayed.

values and correspond to uniform sandy textured soils on siliceous channel sands. A black, NNW-line corresponds on the image to the zone of uplift which has caused ponding of alluvial sands east of the line (appears black in image), and *in situ* deeply weathered sandy soils west of the line (appear green in image). Figure 16a shows the position of the Palmerville Fault (lower right corner of image) and faulting on the Western Plain (lower left corner of image) over the gamma-ray image. The image indicates that the faulting extends further north than interpreted previously (Willmott & others, 1973).

## 10 GEOMORPHIC ACTIVITY/EROSION

Regions where active erosion is taking place can be discriminated on the imagery. Areas of active erosion or stripping of the residual sandy layer and friable saprolite over granite landforms appear in reddish hues (Fig. 4a – central zone of image) because of the high K-feldspar and mica content of the relatively fresh granite beneath. These areas form scalloped patterns on the image, corresponding to low erosional scarps; the depth of stripping is closely related to the depth of weathering. Therefore the gamma-ray imagery can be used as a "geomorphic activity" map to distinguish stable landforms (black/dark blue) with deep weathering and thick accumulations of residual sand (low potassium); from younger landforms (reds) where active erosion and stripping of the surficial cover have exposed relatively fresh granite or saprolite (high potassium). Similarly, areas of active sediment transport (white) and deposition (pink) can be recognised. Accretionary channel and overbank sediments on the coastal plains (in reddish hues, reflecting K-feldspar and mica) can be mapped, and contrast with *in situ* weathering and gradual denudation over the Western Plains (green/blue hues – residual heavy minerals).

## 11 RELATIVE DATING OF SOILS

Variations in potassium, thorium and uranium contents of soils can be used in some areas to estimate relative ages of landforms, and thus can provide an insight into the weathering and geomorphic history of the area.

Investigations in the Ebagoola sheet area show that old stable landforms, where deeply weathered soils have been preserved by low relief and tectonic stability, appear as black and green/blue hues in the gamma-ray image, as a result of the accumulation of quartz and heavy minerals. Old residual bauxitic plateaux are identified by high thorium and uranium signatures due to concentrations of minerals such as zircon and xenotime. Similarly, stable older landforms over granite bedrock can be distinguished from younger, more active areas. Beach ridges can also be categorised into older ridges which consists of quartz sands and appear black in the imagery, and younger ridges which consist of quartz sands and minor mica, and appear in pinkish hues. High thorium response in weathering profiles over EBAGOOLA generally indicates older landforms where deep chemical weathering has occurred; movement of thorium in the landscape appears to be restricted to mechanical transportation. However, these relationships may not apply to other areas: thorium, although stable in a reducing environment, is readily soluble under oxidising conditions. Other regions will show different relationships depending on the bedrock type and on the weathering history.

Mineral weathering indices have for many years been used as a measure of the maturity of a soil or soil horizon. Many of these indices normalise the more soluble mineral components (calcium, sodium, potassium) to aluminium as an index of relative age. However, recent studies

have shown that aluminium in soils is mobile under many environments and can give erroneous results in dating; indices using heavy minerals (zircon) instead of aluminium to date palaeosols formed on silicate rocks have proved more accurate (Chittleborough, 1991). Gamma-ray data, with their ability to show the relative accumulation of heavy minerals may therefore be used to extrapolate dating measurements based on heavy mineral weathering index relationships. A weathering or maturity index of soils over EBAGOOLA can be derived by ratioing the potassium channel with the uranium and thorium channels. High values in the ratioed image generally indicate less weathered younger soils and low values indicate more intensely weathered older soils.

## 12 STREAM-SEDIMENT GEOCHEMISTRY AND GAMMA-RAY DATA

The gamma-ray image(s) may be regarded as a geochemical map showing the distribution of uranium, thorium and potassium in rocks and regolith materials. The ability of the gamma-ray data to show the distribution of transported material including the source rocks from which the sediments were derived, areas of *in situ* weathering, and active and inactive parts of catchments, will provide a complementary data set for aiding the interpretation of stream sediment geochemistry. In addition, the gamma-ray data are able to distinguish structural contacts, geological boundaries, and bedrock types. This information, combined with stream-sediment geochemistry, is potentially very useful for surface geochemical interpretation and modelling.

## 13 IMPLICATIONS FOR GEOMORPHOLOGICAL AND WEATHERING HISTORY

The Ebagoola area has been exposed subaerially since the late Mesozoic, and has undergone continuous weathering and denudation to the present day. During the Tertiary, gently dipping Mesozoic sandstones and siltstones (Gilbert River Formation, Rolling Downs Group), which formed an extensive blanket over the area, were eroded and stripped from the Central Uplands, leaving only isolated remnants. This is evident from the concordant bevelled hill tops on the highest ridges of the Coen Inlier. Drainage systems on the once overlying Mesozoic cover (which probably had quite subdued relief as indicated by the sinuous drainage patterns) have eroded down and are now superimposed on granites and metamorphic rocks of the Coen Inlier. Superimposed drainage, including the west-flowing Little Lukin, Coleman and Holroyd Rivers, can be seen cutting across (steeply dipping) NNW-trending quartzite strike ridges (Fig. 4b). The metamorphic rocks are characterised by moderate to high relief which is mainly the result of differential erosion during the Tertiary.

Downwarping to the east of EBAGOOLA formed the Great Divide and initiated scarp (Great Escarpment) retreat (Ewers & Bain, 1992). The downwarping was probably associated with north-northwest-oriented rifting which led to the opening of the Coral Sea (Weissel & Hayes, 1977). Gradual migration of the Great Escarpment westwards since its initiation has probably occurred mainly by knickpoint retreat followed by valley widening to form lower relief and rounded landforms immediately to the east. As discussed previously (section 9.2), the headwaters of some west-flowing rivers were captured and their flows diverted to the east as the scarp retreated. The Great Escarpment now forms a boundary between the Central Uplands and the eastern Coastal Plains and separates areas of different geomorphic and weathering characteristics.

Landforms west of the great escarpment are generally older (many paleoforms), deeply weathered, and have low geomorphic process rates (erosion and deposition). Landforms east of the Great Escarpment are generally younger, less deeply weathered (fewer paleoforms), and have higher geomorphic processes rates (Ollier, 1982).

The difference between landforms west and east of the Great Escarpment can be distinguished in the gamma-ray imagery. The Western Plains with the exception of modern alluvium along major rivers is characterisied by black and green hues, and contrasts sharply with the eastern Coastal Plain which is dominated by more recent alluvial sediments derived from the central uplands (Fig. 16b). Relatively high thorium and uranium values (with the exception of values associated with metamorphic rocks and sediments derived from them) and overall low gamma-ray values generally indicate old,*in situ,* deeply weathered regolith profiles. These old profiles, some of which have formed during the Tertiary, have been preserved as a result of the low relief and tectonic stability over much of the area. Minor tectonic movements associated with faulting over parts of the Western Plains and along the Palmerville Fault have blocked and redirected drainage. The movements associated with this tectonism was relatively small and did not initiate any major geomorphic activity.

Regolith profile development during the Tertiary has been dominated by *in situ* deep chemical weathering leading to the accumulation of deep residual quartz sands at the surface (black in the image, Fig. 4a, 16b). The underlying bedrock is typically deeply weathered, mottled, and in places, silicified and ferruginised. Induration of alluvium and of the underlying bedrock associated with some valleys on the western plains has lead to differential erosion and drainage inversion (Pain & Wilford, in prep). Tertiary and Quaternary deposits consist of footslope/ colluvium sandy gravels and cobbles, thin sandy and gravely pediments down slope from adjacent hills, and channel and overbank alluvium comprising of clay, sand, gravels and cobbles. In places these deposits have been indurated by clay, silica and iron cements to form duricrusts and hardpans. The type of cement in most cases reflects the bedrock composition; silification occurs mainly on siliceous siltstones on the Western Plains and granitic terrains; clay and iron cementing is more commonly found on the metamorphic terrains and on clayey sandstones on the Western Plains.

## 14 OTHER APPLICATIONS

Soil erosion and salinity have become important factors in maintaining sustainable productivity of agricultural soils in Australia. Gamma-ray data proved to be highly effective in characterising soils of the Ebagoola region by virtue of their capacity to provide a measure of the abundances of primary rock forming minerals, clays and accessory minerals. Areas of active erosion can be delineated where there are differences in the gamma-ray response between the soil and underlying bedrock. Gamma-ray data may also be able to show differences between horizons within a soil profile resulting from weathering and redistribution of mineral constituents (i.e. podzolic soils which has a high degree of horizon differentiation). Thinning or removal of surface soil horizons in areas of land degradation may therefore be identified using gamma-ray data; although this has not been tested and will require further work.

Recent work is beginning to show the application of gamma-ray data in environmental studies. Gamma-ray data have been used successfully for groundwater and salinity studies in the Murray Basin (McDonald & Pettifer, 1992). McDonald and Pettifer (1992) used the potassium channel

to map high-clay soils (high potassium) which correspond to areas of poor water recharge and saline ground waters. Conversely, sandy, low clay-content soils discriminated by low potassium values indicate areas of potential groundwater recharge.

The gamma-ray data therefore provides useful information in effective land management practice and in the prediction and prevention of land degradation. The use of other remote sensing data sets such as Landsat TM have in general been limited to broad land system evaluation and have relied on the type and condition of vegetation as diagnostic indicators for assessing areas of land degradation. Gamma-ray data provide a more direct tool for measuring the properties of surficial materials for soil and land degradation mapping. Gamma-ray surveys will, however, be most effective when combined with other data sets. Integrating and analysing the gamma-ray data with other remotely sensed data sets (i.e. Landsat TM, Spot) and regolith-landform information (AGSO-Regolith Landform Map Series) will provide information to better assess land condition and degradation, and to develop more effective land management models.

# 15 SUMMARY

The use of Landsat TM and high-resolution airborne gamma-ray imagery provides complementary information for geological and regolith terrain mapping.

Adding back the high-frequency component to a three-band (RGB) false-color composite gamma-ray image using the hillshaded/pixel additive method and merging the gamma-ray data with a hillshaded Band 5 Landsat TM scene were effective techniques to enhance and integrated imagery for interpretation. The hillshaded/pixel additive method highlighted local changes in the gamma-ray signal which relate to changes in regolith materials and lithology, and sharpened boundaries associated with morphotectonic features such as the Great Escarpment.

Integrating gamma-ray data with Landsat TM enabled the gamma-ray image to be interpreted in a geomorphological context. Structural and landform information derived from Landsat complemented the gamma-ray image which provided information on bedrock and regolith chemistry.

Although it is possible to distinguish between different lithologies on their potassium, thorium and uranium signatures, higher-frequency and textural variations in the imagery within individual lithologies or lithological groups are related to regolith cover in general, and soils in particular. Distribution of soils, weathering profile characteristics and geomorphic features may be mapped on the gamma-ray imagery, but subtle changes in lithology were effectively resolved on the imagery only when responses due to the overprinting and weathering characteristic of the regolith were known.

The ability of the gamma-ray signal to penetrate through most of the vegetation cover and measure up to 30-40cm of the upper regolith is an advantage over visible/near infrared satellite-sensed data, which are affected by vegetation masking soils and bedrock. Preliminary interpretation of Landsat data was hindered by vegetation, fire-scar patterns (which overprint and confuse rock and soil signatures), and deeply weathered sandy soils which mask much of the underlying bedrock.

Potassium values recorded by the airborne gamma-ray survey relate to major rock forming minerals including alkali feldspars and micas, and to potassium-rich clays such as illite. The potassium channel could be used to gauge weathering maturity of soils and sediments by measuring the relative amount of K-feldspar and mica at the surface. Recent (as indicated by

high potassium values) and old beach ridge sands (low potassium) could be discriminated in this manner. The distribution and concentration of these minerals at the surface are directly related to the underlying lithology, and to the degree and style of weathering. Uranium and thorium occur as trace elements in major minerals such as quartz and feldspar, but occur in much higher concentrations in accessory minerals such as zircon and monazite. High uranium and thorium values in EBAGOOLA are associated with higher-grade metamorphic rocks, garnet-biotite-muscovite leucogranites and pegmatites, and sediments derived from them. High values are also associated with deeply weathered regolith profiles containing heavy minerals (e.g. zircon) in the residual sandy cover. Deeply weathered bauxitic plateaux over parts of the Western Plains, and old residual sandy soils developed over granite in the Central Uplands, are characterised by high thorium signatures.

Deep weathering profiles were generally identifiable in the imagery by high uranium-thorium to potassium ratio, although relationships vary according to the proportions of potassium, thorium and uranium in the bedrock or the transported cover. Low values for all three radioactive elements indicate thick accumulation of residual quartz sand which characterised many of the old, deeply weathered sandy earths in the region.

The imagery can be interpreted as a "geomorphic activity map", showing both stable landforms with deep weathering, and younger landforms with active erosion of the surficial cover. Distribution of *in situ* weathered regolith and transported material, including the source rocks from which the sediments are derived, can also be resolved in the imagery.

The gamma-ray image provided information over a regional scale which contributed greatly to an understanding of the weathering and geomorphic history of the Ebagoola map sheet.

## ACKNOWLEDGMENTS

I would like to thank Dr Colin Pain, Mr Colin Simpson, Mr John Bain and Dr Doug Mackenzie for reviewing and making helpful comments to improve this manuscript. Many thanks to Tas Armstrong for running an efficient field camp and to all the field assistants for their support, and to Dr Colin Pain and Dr John Dohrenwend for assistance in the interpretation and ground checking of the gamma-ray data in the field. Thanks also Dr Peter Milligan and Dr Brian Minty for useful comments on processing the gamma-ray data.

# REFERENCES

Bain, J.H.C., Black, L.P., Blewett, R.S., Bultitude, R.J., Knutson, J., Mackenzie, D.E., Pain, C.F., Wilford, J.R., Dohrenwend, J., Sun, S-S., Trail, D.S., von Gnielinski, F.E., and Wellman, P., 1992 - Cape York Peninsula update. *BMR Research Newsletter*, 16, 18-22.

Briggs, I.C., 1974 - Machine contouring using minimum curvature. *Geophysics*, 39, 39-48.

Chittleborough, D.J., 1991 - Indices of weathering for soils and palaeosols formed on silicate rocks. *Australian Journal of Earth Sciences*, 38, 115-120.

Collins, P.L.F., Wyatt, B.W., and Yeates, A.N., 1981 - A gamma-ray spectrometer and magnetic susceptibility survey of Tasmanian granitoids. *Tasmanian Department of Mines*, unpublished report 1981/41, 68.

Conradson, K. and Nilsson, G., 1984 - Application of integrated Landsat, geochemical and geophysical data in mineral exploration. *Proceedings of the Third Thematic Conference on Remote Sensing for Exploration Geology*, Colorado Springs, Colorado, 499-511.

Darnley, A.G., and Grasty, R.L., 1971 - Mapping from the air by gamma-ray spectrometery. *Proceedings, 3rd International Geochemical Symposium*, Toronto, Ont., Canadian Institute of Mining and Metallurgy, special Vol. 11, 485-500.

Dickson, B.H., Bailey, R.C. and Grasty, R.L., 1981 - Utilizing multi-channel airborne gamma-ray spectra, *Candian Journal of Earth Science*, 18, 1793-1801.

Doutch, H.F., 1976 - The cainozoic Karumba Basin, northeastern Australia and southern New Guinea. *BMR Journal of Australian Geology and Geophysics*, 1 (2), 131-140.

Drury, S.A., 1987 - *Image Interpretation in Geology*. Allen & Unwin, London.

Ewers, G.R. and Bain, J.H.C (eds) 1992 - Preliminary Map Commentary - Australia 1:250 000 Basement Geology and Regolith Landforms: Ebagoola (SD54-12), Queensland. *Australian Geological Survey Organisation*, Record 1992/71.

Foley, J.D., van Dam, A., Feiner, S.K., and Hughes, J.F., 1990 - *Computer graphics, princiles and practice*. Addison Wesley Publishing Company

Foote, R. S and Humphrey, N.B., 1976 - Airborne radiometric techniques and applications to uranium exploration. *In* Exploration for Uranium Ore Deposits. *International Atomic Energy Agency*, Vienna, Austria, 17-34.

Foote, R.S., 1968 - Improvement in airborne gamma radiation data analyses for anomalous radiation by removal of environmental and pedologic radiation changes. In: *Symposium on the Use of Nuclear Techniques in the prospecting and development of mineral Resources, International Atomic Energy Meeting*, Buenos Aires.

Geoterrex, 1991 - Logistic report for an airborne magnetic and radiometric survey, Ebagoola, Queensland, for the *Bureau of Mineral Resources* (unpublished).

Grasty, R.L., 1976 - Applications of gamma radiation in remote sensing, ecological studies, analysis and synthesis. *In* Schanda, E. (ed.), *Remote Sensing for Environmental Sciences*, Springer-Verlag, Berlin, New York, 18, 257-275.

Green, A . A ., 1987 - Levelling airborne gamma-radiation data using between-channel correlation information. *Geophysics*, 52, 11.

Grimes, K.G., 1979 - The stratigraphic sequence of old land surfaces in northern Queensland. *BMR Journal of Australian Geology and Geophysics*, 4, 33-46.

Grubb, P.L.C., 1971 - Genesis of the Weipa bauxite deposits, N.E. Australia. *Mineralium Deposita,* 6, 265-274.

Isbell, R. F and Gillman, G. P., 1973 - Studies on some deep sandy soils in Cape York Peninsula, North Queensland - Morphologial and chemical characteristics. *Australian Journal of Experimental Agriculture and Animal Husbandry*, 13, 81-87.

McDonald, P.A and Pettifer, G.R., 1992 - The application of airborne radiometric classification techniques to salinity studies in Western Victoria. *12th Australian Geological Convention, Ballarat,* 32.

Ollier, C.D., 1982 - The Great Escarpment of eastern Australia: tectonic and geomorphic significance. *Journal Geological Society Australia,* 29, 13-23.

Pain, C., Chan, R., Craig, M., Hazell, M., Kamprad, J., & Wilford, J., 1991 - RTMAP BMR Regolith Database Field Handbook. *BMR record* 1991/29.

Pain, C.F., 1992 - The landscape approach to mapping regolith. *In* Branagan, D.F. and Williams, K.L. (eds), Surface with Geology, Australian LAndscapes and Economic Implications, *Fifth Edgeworth David Symposium*, pp. 45-60.

Pain, C.F and Wilford, J., (in prep) - Ebagoola 1:250 000 Regolith Series explanatory notes, *Australian Geological Survey Organisation record.*

Schaap, A.D., 1990 - Weipa kaolin and bauxite deposits, In: Hughes, F.E.(ed.),*Geology of the Mineral Deposits of Australia and Papua New Guinea,* AUSIMM, Melbourne. 14, Vol 2, Melbourne, 1669-1673.

Simpson, C.J., 1990 - Deep weathering, vegetation and fireburn significant obstacles for geoscience remote sensing in Australia. *International Journal for Remote Sensing*, 11, 2019-2034.

Smart, J., 1976 - The nature and origin of beach ridges, western Cape York Peninsula, Queensland, *BMR Journal Austustralian Geology and Geophysics*, 1, 211-218.

Trail, D.S. and Blewett, R.S. 1991. Noth Queenaldn project 1990 geological reconnaissance of the Coen Inlier, Cape York Peninsula, *BMR record* 1991/99.

Tucker., D.H, Bacchin., M and Almond., R., 1984 - Significance of airborne magnetic and gamma spectrometric anomalies over the eastern margin of the Canning Basin. *In* Purcell, P.G. (ed.), *The Canning Basin, W.A, Proceedings of Geol. Soc. Aust/Pet. Expl. Soc. Aust. Symposium, Perth.*

Welch, R. and Ehlers, W., 1987 - Merging multi-resolution SPOT HRV and Landsat TM data. *Photogrammetric Engineering and Remote Sensing*, 53, No 3, 301-303.

Weissel, J.K. and Hayes, D.E., 1977 - Evolution of the Tasman sea reappraised. *Earth Planet. Sci Lett,* 36, 77-84.

Whitaker, W.G and Gibson, D.L., 1977 - Ebagoola 1:250 000 Geological Series explanatory notes. *Bureau of Mineral Resources, Australia.*

Wilford, J.R., (in prep) - Sampling depths recorded using airborne spectrometric gamma-ray data. *Australian Geological Survey Organisation record.*

Willmott, W.F., Whitaker, W.G., Palfreyman, W.D., & Trail, D.S., 1973 - Igneous and metamorphic rocks of Cape York Peninsula and Torres Strait. *Bureau of Mineral Resources Bulletin* 135.

Yeates, A.N., Wyatt, B.W, and Tucker, D.H., 1982 - Application of gamma-ray spectrometry to

prospecting for tin and tungsten granites, particularly within the Lachlan Fold belt, New South Wales. *Economic Geology*, 77, 1725-1738.

Van Schmus, W.R., 1984 - Radioactivity properties of minerals and rocks. In: Carmichael, R.S. (ed.), *Handbook of physical properties of rocks*, CRC press, United States, 3, 288.